DTU Energy
Department of Energy Conversion and Storage

MANUFACTURE AND CHARACTERIZATION OF ZNO-BASED PHOTOCATALYTIC FILMS

Nadia Hedegaard Arp, s113653

23. JULI 2017
DTU ENERGY
Risø, DTU

Abstract

This report is written as a part of the education MSc. in Chemical and Biochemical Engineering, offered by DTU (Denmarks Technical University) and covers the research subject of manufacturing and characterisation of ZnO based photocatalytic films. The films photocatalytic abilities is documented through degradation of various dyes used in several industries. By degrading dyes through the media of light it is possible to classify the dye degradation as a possible green chemistry, depending on which gasses/compounds are produced during the process.

The paper focuses on thin ZnO films on microscope glass, indicating that the ZnO nanoparticle orientation is random. The research report will cover the manufacturing process, which includes the following parameters: determination of Zn^{2+} concentration in an aqueous solution (MiliQ water), adhesion to the surface of the medium (glass), method of application and calcination temperatures. The project will also cover amount of photocatalyst, defined as cm^2 is necessary for optimal functionality (degradation of dye) to investigate if there is a possible linear relationship between catalytic load and reaction kinetics. Reaction kinetics will be studied in detail, including the influence of the initial concentration of the various dyes.

Studies of morphology of the thin films will be completed by XRD (x-ray diffraction) and SEM (scanning electron microscopy), which will convey if the films are crystalline/armorphous and the possible microstructure of ZnO.

The project focuses on the degradation of blue and blue-green dyes which absorbs light in the range of 600-700 nm. This indicate that while the dyes may depart a similar color to ex. clothing, the structural differences of the dyes may prove challenging to a photocatalyst and impact the reaction kinetics.

Throughout the entire report, it will be evaluated how green the process is compared to no usage of a photocatalyst to degrade the dyes.

Nomenclature

Malachite green oxalate	-	MG
Methylene blue trihydrate	-	MB
Parts per milion	ppm	ppm
Beta	-	β
Alpha	-	α
Poly (ethylene glycol)	-	PEG
Proportional, integral, derivative		PID
Minutes		min
Code of Federal Regulations	-	CFR
Comprehensive Environmental Response Compensation and Liability Act	-	CERCLA
Superfund Amendmendts and Reauthorization Act	-	SARA
Fire and Explosion Index	-	FEI
Chemical Exposure Index	-	CEI
Turn over number	-	TON
Turn over frequency	-	TOF
Rate law constant	min^{-1}	k
Ultra violet	-	UV
Hazard distances	m	HD
Grazing incidence x-ray diffraction	-	GIXRD
Demarks Technical University	-	DTU
Brilliant Green	-	BG
Nano meters	nm	nm
Scanning Electron Microscopy	-	SEM
Field-emission scanning electron microscopy		FE-SEM
Milipascal-second	mPa.s	mPa.s
International Centre for Diffraction Data	-	ICDD
Angle of incident/reflected ray with a crystal plane	θ	θ

Table of content

1 Introduction

Dyes are used in many industries and in large quantities to color products such as textile, cosmetics, leather, paper, plastic etc.. However, the side effect of using dyes as colorants is the wastewater, which often contains high concentrations of dyes. The colored wastewater affects the transmissions of sunlight into streams and thus reduces photosynthesis. Moreover, the dyes may be toxic to microorganism and/or carciogenic to mammals. To complicate it further dyes are poorly biodegradable (Sartape, et al., 2014). Thus, it is relevant to find an alternative to degrade dyes in wastewater.

It has been estimated that more than 10000 different dyes/pigments are used in the industry, and that moore than $7*10^5$ T of synthetic dyes are produced anually worldwide. From the textile industry approxiamtely 20000 T of dyes are lost to effluents each year during the process, due to inefficient dying processes. Many of these dyes is not removed from conventional wastewater treatment even though an environmental legilislation is in place to eliminate color from effluents before disposal into water bodies. This is due to the dyes stability to light, temperature, detergents, chemicals etc. (Chequer, et al., 2013).

The textile industry alone uses a lot of water, and the wastewater from these plants are classified as the most polluting in the industrial sector. It has been estimated that the loss of color in the dying operation to the environnment can reach 10-50% (Chequer, et al., 2013).

Metal oxides are suitable for photocatalysis since they have significant photocatalytic features such as desired band gap, suitable morphology, high surface area, reusability and stability. Having these charactersitics allow metal oxides to have similar photocatalytic processes such as light absorption, which causes a charge seperation process (Khan, et al., 2015). ZnO is such a metal oxide.

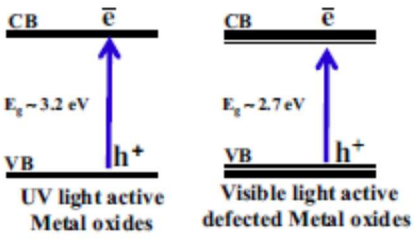

Figure 1: Metal oxides showing possible excitation (Khan, et al., 2015)

ZnO has a bandgap of 3.2 eV and has interesting optoelectriccatalytic and photochemical properties. Furthermore ZnO has superior quantum efficiency and absorbs a larger fraction of the solar spectrum compared to its competitor TiO_2, since they have a similar band gap. Thus, ZnO is the optimal choice for photocatalytic degradation, even if TiO_2 is more effective (Lu, et al., 2009). ZnO is a semiconductor belonging to II-VI semiconductors with a high binding energy of 60 meV and can be synthesized from a varietyof methods and from well.defined nanostructures such as nanospheres, nanorods, nanowires etc. (Saravanan, et al., 2013).

ZnO is a heterogenous photocatalyst which has been proven succesfull and efficient in degrading pollutants in water into biodegradable products and eventually mineralisating the pollutants int CO_2 and H_2O (Khan, et al., 2015).

2 Theory

2.1 Dyes

Dyes are classified as chemical able to bind to fabrics and impact a color. There are several categories of color, where malachite green is identified to belong in triphenyl methane category according to (Raval, et al., 2016). They are used in quite a few industries in large amounts as a colorant of products. This need of color will be a part of the waste water, which affect the transmittance of sunlight to living organism in the water, and reduces the photsynthetic reaction. It will also influence all animals drinking from that water, which may lead to carcinogenic effects or directly toxic, see Table 2. MG (malachite green) is used to color leather, wool, jute and silk, in distilleries to kill of fungus and in aquaculture industry to fight parasites and diseases (Sartape, et al., 2014).The triphenylmethane category belongs to electronic origins of color as displayed in Figure 2. The category is based on the electronic mechanism used to create the color, which is sectioned into four groups: (1) Donor-acceptor chromogens (2) Polyene chromogens (3) n->Π^2 chromogens (4) Cyanine type chromogens (Raval, et al., 2016).

A triphenylmethane category as shown in Figure 2 is based upon dyes which are based on triphenylmethane and has an intensely color, synthetic fabrication and is sensitive to light.

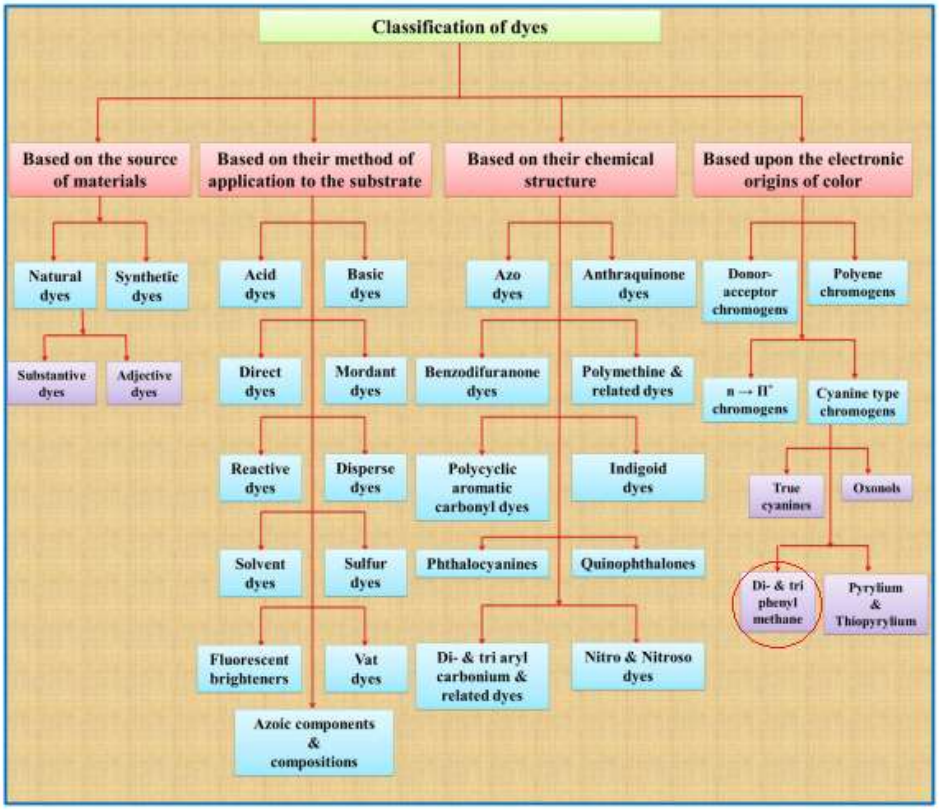

Figure 2: classification of dyes as according to (Raval, et al., 2016). The red circle indicate the triphenyl methane group where MG belongs

MB (methylene blue) is not a triphenyl methane dye, since the structure does not contain a triphenyl, instead it is a phenothiazine dye/thiazol dye, which is often used in medical treatments combined with light (pubchem, 2017). This however, makes it resistant to light treatments, but it has been proved by (Mohabansi, et al., 2011) and (Balcha, et al., 2016) that it is possible to degrade MB under UV irradiation by the usage of TiO2/ZnO and ZnO nanoparticles, respectievely. If MB should be classified according to Figure

2, it will belong to either azo dyes or sulphur dyes, which are the most common dye groups. Azo dyes is the largest groups of dyes and consist of 60-70% of all dyes produced (worldwide), due to high molar exctinction coefficient, great structural diversity, medium-to-high fastness properties related to light and wetness (Chequer, et al., 2013).

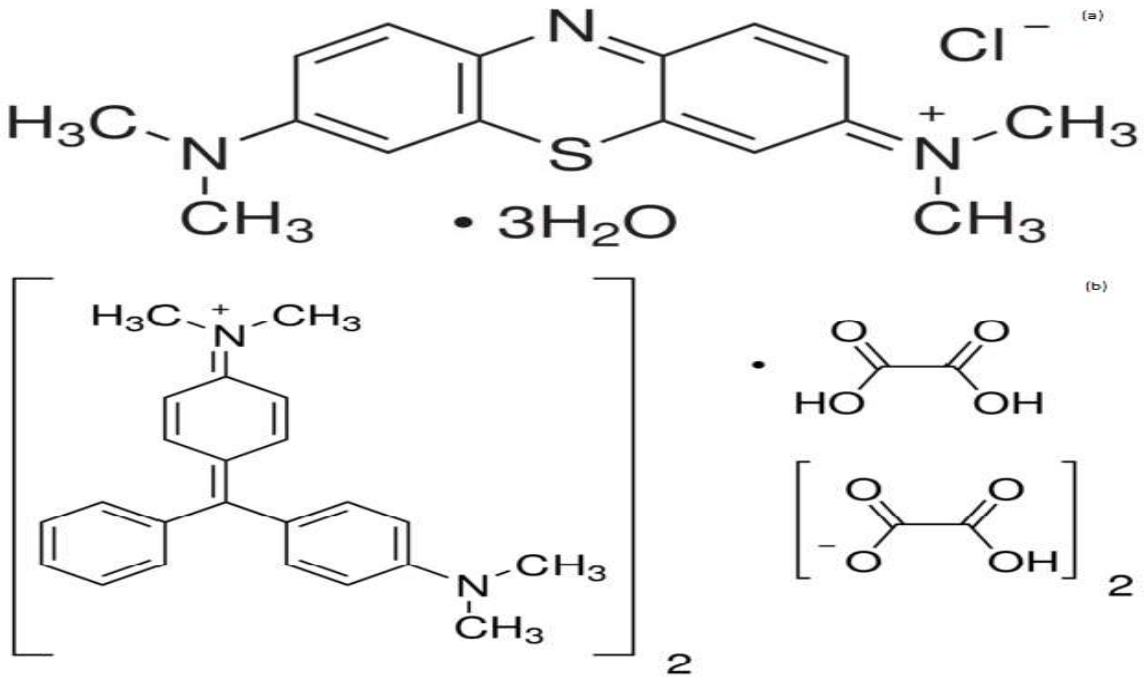

Figure 3: (a) structure of MB (b) structure of MG

The different structures of MB and MG is observable in Figure 3, where it quickly becomes apparent, that MG has a triphenyl group, whereas MB has a N=N and sulphide. It may indicate that the degradation of the different dye groups differs, thus some dye groups may be more succesible to degradation than others, depending on the microstructure and whether or not that energy gap can be overcome. It has been noted in a research paper that MG is degradable by thin ZnO films (Stambolova, et al., 2014), however no such paper was found for MB. This may indicate that it is not possible or have not been researched. The different structures indicate that the degradation happens differently for each dye category, and that there may not be an universal catalysts to degrade all categories, since catalysts are specific.

MB and MG do have some structural similarities. Both have the same functional group NC_8H_{11}, which is a dimethylaniline functional group and is often used in the dye industry as an intermediate during the maufacturing. Dyes with such functional group is created through an reaction with R-Mg-X to complete a Grinard reaction. A Grinard reaction is an addition reaction, where no water is present, and new carbon-carbon bonds are formed (Mortimer, 1975). It is possible to synthesize MG through such a reaction:

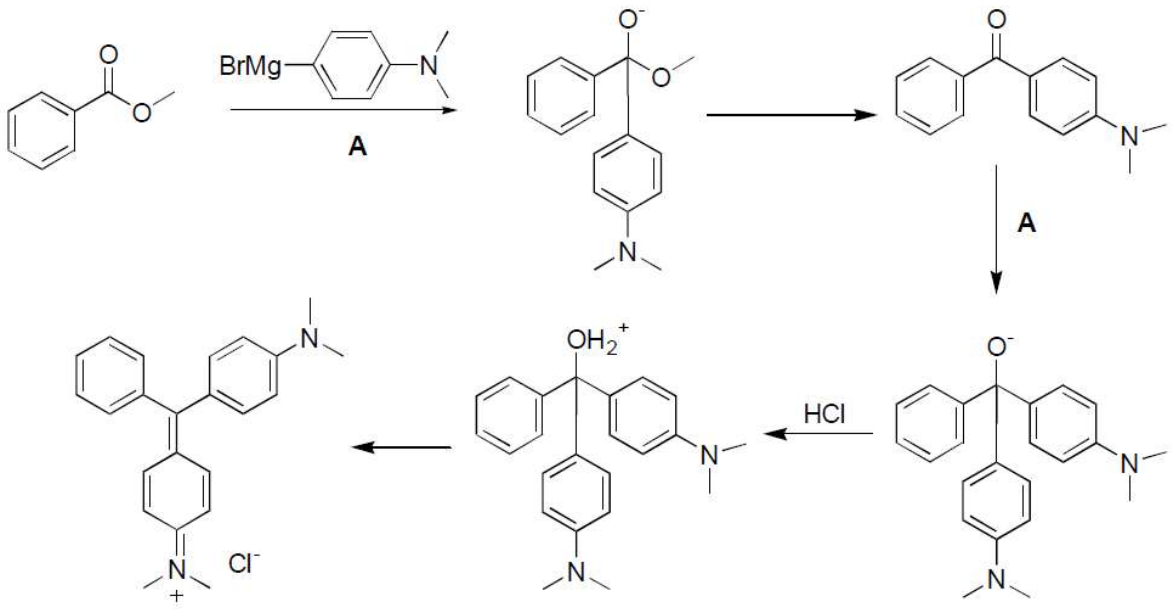

Figure 4: Synthesis of MG through Grinard reagents (Wake Fores University, Chemistry 223L, 2017)

The synthesis of MB is different due to its structure of three connecting benzene rings. It is possible to synthesise MB by the following reaction scheme:

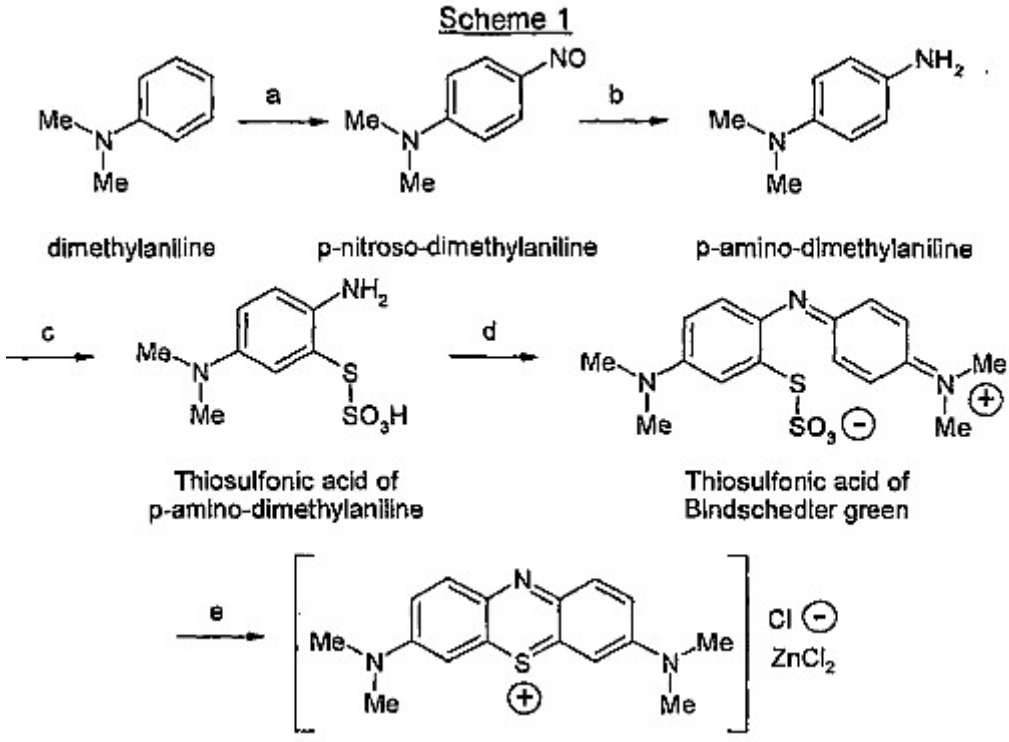

Figure 5: Synthesis of MB (Ltd., 2011)

It is possible to synthesise MB by starting with a dimehtyl aniline and reacting it with $NaNO_2$ in HCl(aq) and get nitrosodiummethylaniline (a) which is then reduced (b) and oxidised (c-e) causing the closure of the ring structure (Ltd., 2011).

It is a difficult task to remove color from wastewater, since dyes are designed to resist biodegradation, and thus remain in the environment for a long time. An example is the half life og 46 years (pH 7, 25°C) for hydrolyzed Reactive Blue 19. According to the legilislation surrounding effluent discharge, there is no official paper stating the limit values for different countries. Federal countries and european have established limits which must be fulfilled, however countries such as India, Malaysia and Pakistan levels are recommended but is not mandatory (Chequer, et al., 2013).

2.2 Photocatalytiz ZnO

Photocatalysis is a term of two words, catalysis which accelerates a reaction without being consumed and the usage of light under which the catalyst is activated.

To be more specific, catalysis only influences the rout to equilibrium, and it is only about reaction kinetics. The raction kinetics deals with the way of moving from A->B, whereas thermodynamics deals with the 'elevation' from A->B., thus a catalysis does not influence the thermodynamics of a reaction.

Since there can be many reactions, which involves one or more rectants/products, there is an equal amount of rate laws. The rate laws are describes as zero-order, first-order and second-order rate laws which comprehends the most common reaction types. Then there are the less common ones, such as Langmuir-Hinselwood kinetics for heterogenous catalysis, Michaelis-Menten kinetics and so on (Rothenberg, 2008).

(Stambolova, et al., 2014) observed that for ZnO film the reaction kinetics were a pseudo-first order reaction kinetics and for vanadium doped ZnO it was found, that it followed a Lagergren pesudo-first order kinetics (Khezami, et al., 2016).

Some of the most important measurements of catalytisis is TON (turn over number) and TOF (turn over frequency) which deals with how many cycles a catalyst can be used before deactivation and TON/time, respectively (Rothenberg, 2008).

To be more specific, photocatalysts is a compund which produces electron-hole pairs when absorbing light and induces chemical transformations in the dyes. The photocatalysts then undergo regeneration to the prior electronic state (Jo, et al., 2014).

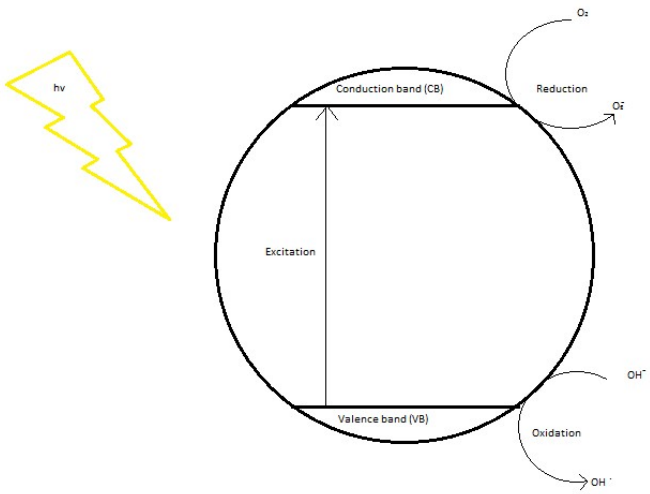

Figure 6: CB indicates excitation of the electrons causing a reduction. VB is the H+ which causes oxidation. It is possible for both the reduction and oxidation to degrade dyes

Figure 6 illustrates the catralytic circle of ZnO, where the excitation covers the bandgap of 3.2 eV which allows energies of UV-VIS (ultra violet visible) light (<387 nm) to cause electron-hole pairs. Meaning, that when sufficient photons (light is both wave and photons) hits the surface os a semi-conductor such as ZnO, an electron is excited out of its valence band and jumps up to a higher energy state, leaving a electron-hole behind in VB (valence band). This leads to degradations on the surface of the semi-conductor through redox reactions (Jo, et al., 2014).. In the process ZnO is activated by UV-VIS light and photoexcited electrons jumps from the valence band to the conduction band, thus forming an electron hole pair of e^-/H^+. The electron hole pair is able to reduce or/and oxidize organic compounds on the surface of the photocatalyst. The activity of the photocatalysis is attributed to the generation of OH° radicals through oxidation (as shown in Figure 6) of OH^- anions and the generation of O_2° radicals. It is important to note that both radicals and anions can react with the dyes and degrade/transform them into less harmfull products (Khan, et al., 2015).

2.2.1 Orientation of ZnO

It is well-known from material science that ZnO is a nano-material due to its particle size where properties may depend on the size, where the effects may appear as quantum mechanical and others related to surface phenomena (Callister & Rethwisch, 2011).

What there has not been thorougly investigated, is the influence the choice of substrate has on the orientation ZnO nanoparticles. (Taabouche, et al., 2013) completed such an investigation by growing ZnO on various substrates which were grown by pusled laser deposition (oxygen pressure ˜1 Pa). It was noted that Figure 7 emerged, which indicate that Si with known lattice parameters only gave one signal in GIXRD (grazing incidence x-ray diffraction).

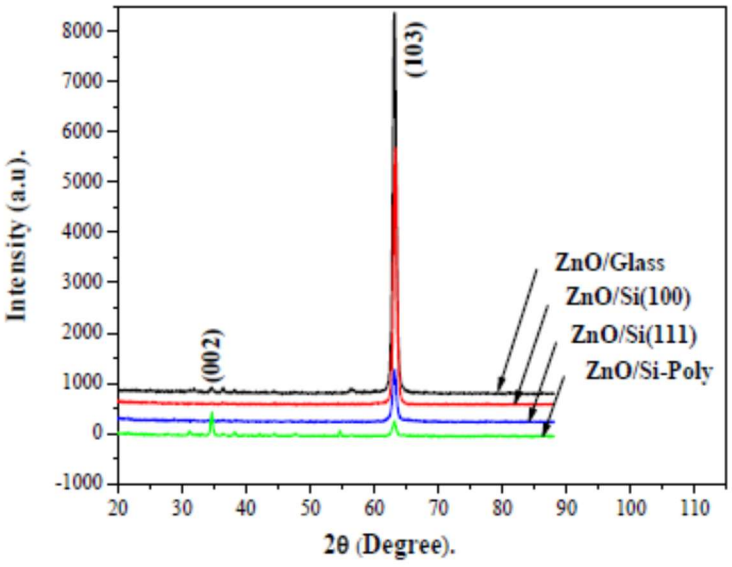

Figure 7: GIXRD of thin ZnO films on various substrates (Taabouche, et al., 2013)

It was also noted that glass gave various peaks, which indicate a random orientation of ZnO on the subtrate. GIXRD also shows that ZnO films has a hexagonal wurtzise structure (polycrystalline) with a strong (103) orientation (c-axis preference), no matter the substrate and has a good crystallinity on monocrystalline Si(100).

The choice of substrate is important since it influences the growth of films due to lattice and thermal mismatching between ZnO and the substrate, since it leads to stress in the film. It is known that strain affects the conduction bands of Ge, Si and gap III-V semiconductores differently (Taabouche, et al., 2013).

However it has also been noted that pulsed laser deposition with different oxygen pressures (50 ,100 ,500 Pa) gives the film layer a random orientation, more orientation peaks and a decreased crystalline quality.

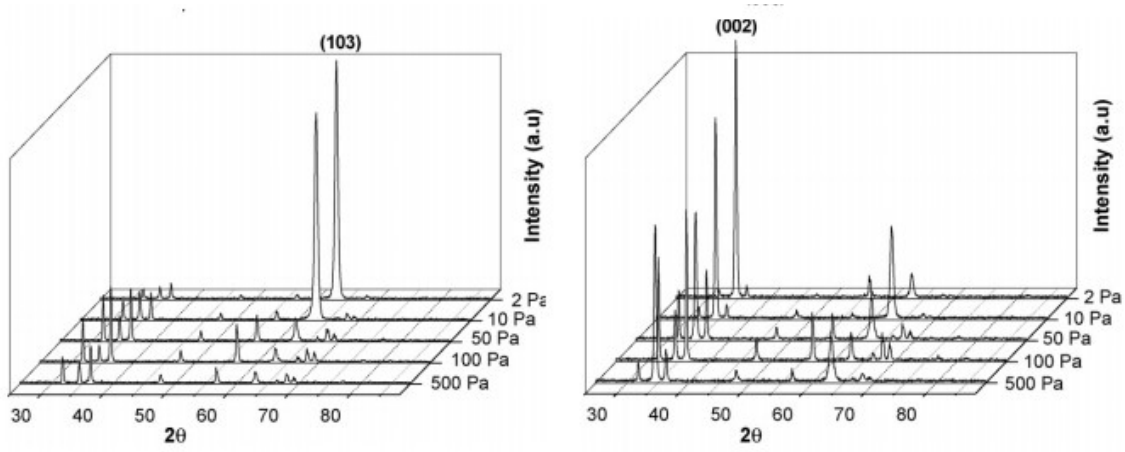

Figure 8: left: ZnO/glass right:ZnO/Si (Lemlikchi, et al., 2010)

Figure 8 illustrates the differences between the substrates. It is apparent that the preffered orientation on a glass substrate is (103), however further peaks are shown, giving the ZnO film layer a random orientation. For Si substrate (001) the prefered orientation is (002) where again number og orientation peaks decreases/drops with an decreasing oxygen pressure (Lemlikchi, et al., 2010). From these results it is shown that orientation do depend on substrate choice (and its orientation) and oxygen pressure.

2.2.2 Methods to obtain ZnO

There are several methods to obtain ZnO, which require different processes and different chemicals. Some processes are less green than others and is not examined further in this paper. The methods can be seperated into several main techniques where each have sub-units which provides different microstructures (nanorods, rods, flakes, hexagonal etc.). The main processes can be listed as: mechanical, precipitation, precipitation in presence of surfactants, sol-gel, solvo-thermal, hydrothermal, microwave, emulsion and microemulsion. Some of the processes require only one chemical whereas other require 5 or more (Kołodziejczak-Radzimska & Jesionowski, 2014).

The applied methods involves a decomposition of zinc acetate dihydrate. (Sing, et al., 2014) analyzed thermal behaviour of zinc acetate dihydrate (under nitrogen flow) in the temperature range of 30-500°C and came forth with:

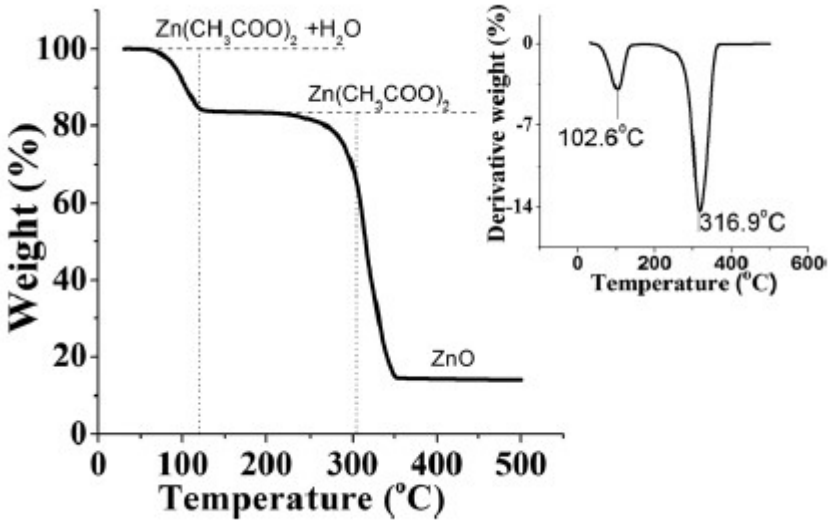

Figure 9: Thermal behaviour of zinc acetate dihydrate and the first derivative of the TG thermogram (Sing, et al., 2014)

Which indicate that to achieve ZnO through thermal decomposition from zinc acetate into ZnO occurs at 316-353°C, and beyond this temperature and up to 500°C formation of stable ZnO crystal ensues. (Sing, et al., 2014) This indicates that the calcination temperature should at the lowest be 400°C. These temperatures are fairly consistent with the ones expresssed in (Kołodziejczak-Radzimska & Jesionowski, 2014) for varying methods. However, some methods require lower temperature due to a different starting point and chemicals.

Figure 9 indicates that different temperatures produce diferent zinc structures. Several scientific papers uses different temperatures to obtain ZnO. This is examined in (Li & Haneda, 2003) where organo-zinc hydrolysis is examined at different temperatures. It was discovered that there were a relationship as shown in Figure 10:

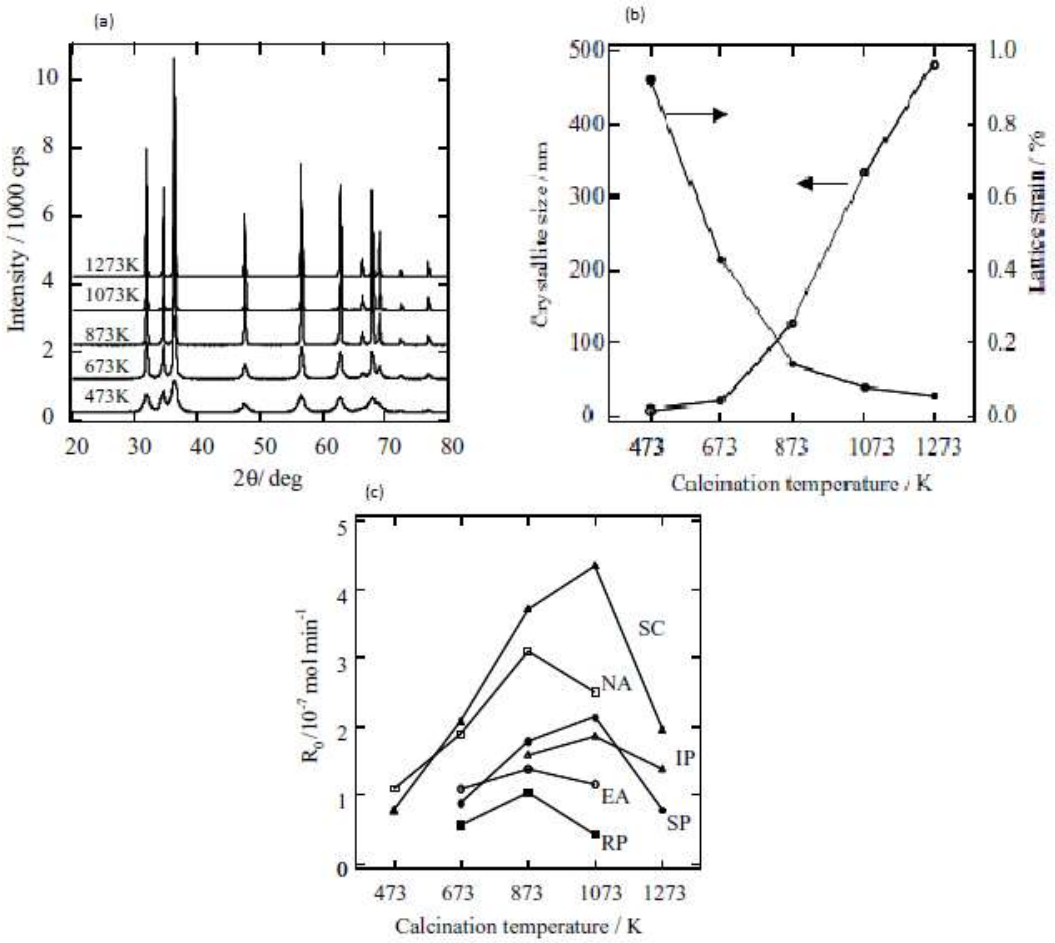

Figure 10: Results from (Li & Haneda, 2003). where (a) and (b) illustrates the same crystalline structure SC and (c) is the catalytic activity for different ZnO structures expressed by initial rate of CO2 formation

Figure 10 clarifies the relatationship between calcinatation temperature,crystalline size and intensity in XRD. Here it becomes apparent that the crystalline size may only become a certain size, before it effected the catalytic activity due to surface area decreasing. Thus, it is important to examine the calcination temperature parameter in order to properly express the best catalytic activity for the decomposition of the dyes.

(Yuan, et al., 2014) have examined ZnO nanostructure formation during oxidation of Zn substrate surfaces in the temperature of 400-1000°C gives different nanostructures. The range of temperature covers the melting (420°C) and boiling temperature (907°C) of Zn.

(Yuan, et al., 2014) found that at low temperatures (200-300°C) no ZnO was formed, but when the temperature was increased to 400°C, ZnO nanowires was produced. As the temperature increases the morphology of the ZnO nanowires changes and becomes more rough and tapershaped and at 800°C ZnO rods are formed. (Yuan, et al., 2014) also examined Si, where ZnO nanostructures are deposited onto Si wafer due evaporation of Zn and subsequent reaction with oxygen. No microstructures below 500°C was found, but in the range of 500-800°C thin ZnO films were created, thin discontinious ZnO film layers were produced on the Si surface, and the films became more continious at higher temperatures.

This all suggest that the formation of ZnO nanostructures are temperature and method dependend as observed in (Kołodziejczak-Radzimska & Jesionowski, 2014), where many methods, temperatures and nanostructures are compared.

The method used in this paper is Zn deposition on a glass surface which receives thermal treatment at or above 400°C.

(Nehru, et al., 2012) used a zincacetate solution and spray pyrolysis to produce thin ZnO film layers on a glass surface (microscope glass). It was discovered with the spray pyrolysis temperature of 300°C that the ZnO distributed on the glass surface appeared to be small grain-shaped structures. And with increasing annelaing temperatures (400-450°C) the grains have increased in size, credited to crystalline growth due to heat treatment. It was noticed that the morphology changed when the samples were annealed. The annealed samples had grain agglomerations, ZnO islands, very tall features and smooth surfaces. Furthermore, the thickness of the film has a great influence on the quality as an oxide semiconductor, since the thickness modifies atomic orientations, defect structures and optical properties. Electrical transport properties depend on the films grain size, shape, defects etc. and electrical resistivity, Hall mobility and carrier concentration depends on the film thickness. Thus it is important to ensure that every produced catalyst in this paper happens under the exact same conditions.

2.3 Handling of chemicals

It is important in any chemical industry to understand the applied chemicals, and how they should be handled, stored, and in case of emergency procedures. All of this is needed if a scale-up is necessary, thus it is relevant to read up on DOW CEI Index (Chemical Exposure Index) and Sereveso Directive III.

DOW CEI Index deals with leakage of chemicals, thus it is important to know, which chemicals is present in which amounts and combined with FEI(fire and explosion index) it is possible to estimate best distances between chemicals themselves and the human population. For example, if ethanol is stored in a 100 L tank at ambient temperature and pressure and ruptures a 5 mm hole in the bottom HD-1 (hazard distance)and HD-2 will be 103 m, 76 m, respectively with a CEI of 7.6, see Appendix 3: CEI calculation for ethanol for calculations.

Table 1: Inventory of chemicals needed to create thin ZnO film layers

Name	Cas number	IUPAC name	Formula	boiling point	storage	density	solubility in water	phase transition	Source
Zinc acetate	557-34-6	zink(II) acetate dihydrate	$C_4H_6O_4Zn*2H_2O$	~200°C	hood, store at room temperature	1.84 g/cm3 at 25° C (lit.)	430 mg/mL	solid-liquid	(scbt, 2017)
Malachite green oxalate	2437-29-8	Bis[[4-[4-(dimethylamino)benzhydrylidene]cyclohexa-2,5-dien-1-ylidene]dimethylammonium]oxalate, dioxalate	$C_{23}H_{25}N_2 \cdot C_2HO_4 \cdot 0.5C_2H_2O_4$	144-150° C	store at room temperature		60 mg/mL (blue to very dark blue)	solid-liquid	(sigma-aldrich, 2017), (scbt, 2017)
Methylene blue trihydrate	7220-79-3	[7-(dimethylamino)phenothiazin-3-ylidene]-dimethylazanium;chloride;trihydrate	$C_{16}H_{18}ClN_3S \cdot 3H_2O$	100-110°C (decomposes)	Store at room temperature	0.98 g/mL at 25 °C	43,600 mg/L at 25°C.	solid-liquid	(pubchem, 2017), (chemical book, 2016)
Ethanol	64-17-5	Ethanol	CH_3CH_2OH	78.29°C	store at room temperature in a tightly closed container away from flash points	0.7893 g/cu cm at 20 deg C	1000000 mg/L (at 25 °C)	-	(pubchem, 2017)
Acetone	67-64-1	propan-2-one	C_3H_6O	56.08°C	store at room temperature in a tightly closed container away from flash points	0.7845 g/cu cm at 20 deg C	1000 mg/mL at 25 °C	-	(pubchem, 2017)
Poly (ethylene glycol)	25322-68-3	ethane-1,2-diol	$HO(C_2H_4O)_nH$	>150 C	No specific storage temperature	1.124 g/cm3 (20 °C)	70 g/l soluble	-	(Merck, 2017)

As Table 1 indicates, several of the liquid components are dangerous if it comes in contact with ignition, since they are volatile solvents. Furthermore Mili-Q water is necessary in the process as a solvent to zinc acetate dihydrate, which means if a scale-up is planned, a water purification facility is needed. Furthermore, it is important to know how toxic the chemicals are to humans and the environment as displayed in Table 2, if it wants to be classified as a green process. The most volatile is ethanol and acetone which are used to clean the glass before production of film layer. The two solvents effect the skin and can cause burns in the respiratory system if inhaled. Thus it may be critical to have gas detectors present at production site and temperature measurements in the storage area. Furthermore, escape plans are needed since it will only take a spark to ignite some of the fluids.

It is known that the US government does not allow higher levels than 750 ppm in laboratories, however most people will smell acetone at 100-140 ppm, meaning acetone is smelt long before it affects the body (U.S. Department of Health and Human Services, 1994).

Acetone is found naturally in the nature and living organism but high amounts (if ingested) may lead to dead or serious inhalibiation, thus is it a good idea to ensure collection of spilled acetone, so that only a limited amount escape to the soil and atmosphere. An idea would be to have a spill-chamber (made of ex. concrete) underneath the storage container in case of liquid leakage.

MG as indicated in Table 2, is toxic to aquatic life and high amounts must not be present in water in order to minimize a negative environmental impact.

MB possess an ability to cause damage to organs through a prolonged or repeated exposure, such as it being present in the drinking water (pubchem, 2017),thus in developing countries it is important to remove it from the wastewater. MB does not fall under the clean water act (U.S.) due to Clean Water Act 40 CFR 122.21 and CFR 122.42, nor does it belong under CERCLA 40 CFR 302 or SARA 40 CFR 355 (VWR, 2016), since it is currently unknown how it influences the environment.

Table 2: Toxicology of chemicals applied and how to handle them

	Characteristic			Indication to environment	Handling	
	Physical	**Chemical**	**Toxicological**		**Normal**	**Accident**
Malachite green oxalate (Pro-Lab Diagnostics, 2016)	-solid,: green crystals -liquid (in water) blue	-flammable liquid and vapor -alcoholic odor -thermal decomposition or combustion may include CO_2, CO, NOx and hydrocarbons	-if large concentrations is inhaled it will lead to dizziness and drowsiness -ingested leads to discomfort -cause mild skin irritation, prolonged contact may cause irritation and dry skin	-harmful to aquatic life with long-lasting effects	-keep away from higher temperatures and ignition sources -use gloves and eye protection -work in well-ventilated area	- in case of fire use foam, carbon dioxide, dry powder or water fog -vapors may be ignited by a spark -if leakage has occurred use water spray to disperse vapors
Methylene blue trihydrate (pubchem, 2017)	solid: green crystals -liquid (in water) blue -odorless	-inhibits guanylate cyclase and treat cyanide poisoning -when decomposed it can emit toxic fumes of NOx, SOx and HCl - is likely combustible	-stains negatively charged components in cell, to locate tumor during operation -large of amounts ingested may produce nausea, vomiting, abdominal pains, precordial pains, dizziness, headache, hypertension, sweating, confusion -can cause damage to organs through prolonged or repeated exposure	-germicidal -unknown hazards to aquatic environment (VWR, 2016)	- have filter respirator nearby -use goggles -use gloves	-In case of fire use a dry chemical (carbon dioxide or halon) -in case of leakage use absorbent material to soak it up, after dilution with water
Ethanol (pubchem, 2017)	-transparent liquid at room temperature -soluble in water	-has odor threshold of 10 ppm	-can cause skin and eye irritation and is confirmed animal carcinogen with unknown relevance to humans. -irritation eyes, skin, nose; headache, drowsiness, lassitude (weakness, exhaustion), narcosis; cough; liver damage; anemia; reproductive, teratogenic effects		-ensure that breathing apparatus is nearby -do not apply heat to it, due to toxic gasses being released -keep away from ignition points -use gloves	-evacuate area and wait for worst fumes to evaporate -in case of fire, evacuate area
Acetone (U.S. Department	-colorless liquid -evaporates in air	-distinct smell and taste -at 100 to 140 ppm, it can be	-The liver breaks down acetone to chemicals that are not harmful if acetone enters the body. The	-Acetone ensues naturally in plants, trees, volcanic gases, and forest fires	-ensure that breathing apparatus is nearby -use gloves	-In case of serious symptoms occurring contact the nearest hospital

	Characteristic			Indication to environment	Handling	
	Physical	**Chemical**	**Toxicological**		**Normal**	**Accident**
of Health and Human Services, 1994)		smelled and is detectable in water at 20 ppm.	amount not broken down leaves the body in the exhale -may cause irritation to nose, throat, lungs and eyes at 100 ppm -may cause headache, lightheadedness, dizziness, unsteadyness and confusion at 12000 ppm -swallowing acetone cause unconsciousness -may cause skin irritation if prolonged exposure	-acetone can react sith sunlight -average time for acetone in the atmosphere is 22 days -microbes can remove acetone from soil -is present in water for less than a day -gives similar symptoms to animals if exposed, some cases led to death	-keep away from ignition points	-evacuate area and wait for worst fumes to evaporate -in case of fire, evacuate area
PEG 200 (pubchem, 2017)	-Clear, colorless, syrupy, odorless liquid -Is combustible at or above 200 F must be preheated before ignition can occur	-sweet taste. -- When heated to decomposition it emits acrid smoke and irritating fumes -On combustion, forms toxic gases. Reacts with strong oxidants and strong bases	-poisonous if ingested - By ingesting large quantities causes central nervous system depression, cardiopulmonary effects and renal damage. -exposed to low levels of ethylene glycol by inhalation for ~ a month were throat and upper respiratory tract irritation	-hazard is mostly environmental since it can seep into the soil and leads to contamination	-Use gloves, and not near high temperature equipment	-Remove it by diluting it with water due to stickiness qualities of material. Use a solvent to remove leftovers. -small fires should be extinguished with carbon dioxide or dry chemical extinguishers and large fires with "alcohol" type foam extinguishers. -use filter respirators if gas is present

From Table 1 and Table 2 it can be concluded that for an scale-up to work, it requires a well-ventilated area vast enough so that explosive chain reactions will not happen in the storage area. Furthermore a cleaning system of the glass is needed since it involves fumes of acetone and ethanol, which have negative side effects to human health if breathed in over a longer period of time.

Methodologies

Several methodologies have been applied during the course of this project. Some of them deals with identification of materials, other with parameter estimation and concentration changes.

2.4 Dip coating

A dip coating method is used to apply a thin film layer on the glass. Several parameters (viscosity of solvent, speed etc.) is involved in this process which have been thoroughly examined.

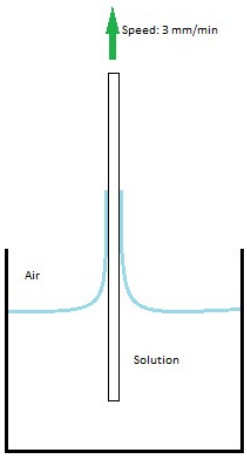

Figure 11: An example of the dipcoating process, showing the possible adhesion to the surface

Dip-coating is a steady-state withdrawal from a liquid which was described by Landau and Levich in 1942. Dip-coating is the most simple coating process to date, where film thickness is dependent on withdrawal speed, gravitational accelerarion, properties of the liquid. The most important aspect of film coating is the surface forces has to dominate viscous one to make the film stick to the surface (Schwartz & White, 1994), (Krechetnikova & Homsy, 2005).

The viscosity is examined by addition of a thickener such as PEG. PEG 200 has a viscosity of 60 mPa.s (Sigma Aldrich, 2017)) at 20°C, thus increasing the degree of stickiness to the glass and giving the solvent a chance at evaporating.

The speed of the upwards moment is examined by having a fixed concentration and a varying speed and observing how well the film layer sticks to the surface. If the speed is to high it is not possible to form a film layer, if it is too slow, it is an inefficient usage of time.

2.5 XRD

X-ray diffraction (XRD) is used to identify ZnO films on the glass substrate by identifying crystalline phases and estimates particle sizes.

The basis of diffraction is that a atom/scattering is hit by electrons/neutrons that have wave-like properties, and when two atoms are close to each other the wave-fronts emerging will overlap and lead to

interference which is dependend on the distance between the two atoms, resulting in a possible detectable lattice structure (Rankin, et al., 2013). As the x-rays hits the catalytic sample it is diffracted by the crystalline phases as according to Bragg's law and that the intensity of the diffracted x-rays is given as a function of the diffraction angle and sample orientation (diffractogram) as shown in Figure 7 and Figure 8. It is the diffraction patterns which allows identification and measures of the size and lattice spacing of the crystallites. If a sample is unknown its diffraction patterns is identifiable trhough XRD since it can be compared to the ICDD (International Centre for Diffraction Data) database.

It is important to notice that noncrystalline catalyst will show either a broad and weak diffraction lines or no diffraction at all. An alternative is to study the morphology of the layers by electron microscopy by applying Field-emission scanning electron microscopy (FE-SEM) (Sanzaro, et al., 2016).

2.6 UV-VIS spectophotometry

Applied to identify absorption of light of the two dyes (MB and MG).

It is well-known that different chemicals absorb light at different wavelength uniquely to them. Thus determining the wavelenght of maximum absorption can be used to observe concentration drops in the presence of the ZnO catalyst.

The absorption in the ultra violet area, depends on the chemical structure of the compounds by exitation of electrons in the ground state to a excited state (higher energy state). The energy absorption inclines a change in electronic energy of a molecule caused by transitions of the valence electrons from an occupied orbital (nonbonding p or bonding π orbital) to the next higher energy orbital (antibonding π^* or σ^*) as indicated in Figure 12:

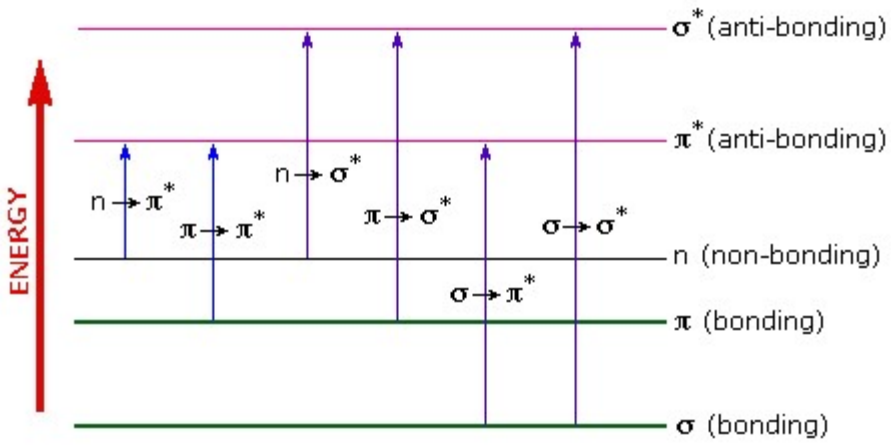

Figure 12: Energy level diagram (William Reusch, 2017)

Figure 12 shows the possible transitions to excitation which may occur in organic molecules. Only the n->π^* and π->π^* is achieved by energies in the range of 200-800 nm. According to (Cennens, et al., 1988) MB absorbs at 664 nm and MG absorb at 618 nm (Stambolova, et al., 2014).The excitation always occurs as an electron promotion from the highest occupied orbital to the lowest unoccupied orbital, and the result of the promotion is known as the excited state.

When a molecule is exposed to light at en energy level which matches a possible electron transition, some of the light energy will be aborbed, thus promoting the electron transition to an excited state. This is measureable in UV (ultra violet) spectroscopy (Silverstein, et al., 1991). The energy absorbed by the

molecule is given by the relationship between Planck's constant and the frequency of the radiation (relationship between speed of light and the wavelength) (Rankin, et al., 2013).

The intensity of the absorbtion can be used as quantification of the actual concentration in a solutions, since it has to follow Lambert-Beers law.

2.7 Scanning electron microscopy

By using SEM (scanning electron microscopy) it is possible to magnify images to a few nanometers and allow study of said images, by allowing a high-energy electron beam to be scanned over a small area of the sample. This causes the generation of low-energy elecrons, which escape from the surface and is detected due to an attraction to the phosphor screen, thus allowing a photomultiplier to measure the light intensity.

It is possible to achieve a 3D image of the surface of the ZnO catalyst since some of the beams electrons are bounced back and give information on the toppography, and with combination of the measureable low-energy electrons the 3D image is created (Rothenberg, 2008).

3 Experimental

This section of the papaer focuses on the experimental issues, such as tuning parameters (Zinc concentration, dipping speed, drying, calcination temperature and time etc. It is relevant to investigate such parameters, since the microstructure may not change but intensity in XRD patterns may change as a function of calcination temperature. (Li & Haneda, 2003) investigated calcination temperature as a function of photocatalytic activity and discovered that calcination temperatures influence photocatalytic activity.

3.1 Materials

Zinc acetate dihydrate $Zn(CH_3COO)_2*2H_2O$ (>99.5%), milli-Q water used as a solvent, PEG 200 used as a thickener, ethanol (>99%) and acetone used to clean the glass, malachite green oxalate (2437-29-8) and methylene blue trihydrate (7220-79-3).

3.2 Sample preparation

A 0.8 M solution of zinc acetate is prepared and stirred at 400 RPM until all zinc acetate dihydrate is dissolved. 19 mL of PEG 200 is slowly added and it is stirred for several hours until a transparrent/misty liquid is required. See 7.2 for further details of concentration determination and PEG amount.

The glass is washed in acetone and ethanol and dried in the oven at 150°C for 15 minutes. When cooled, dip coating technique is applied at a velocity of 1 mm/min. It is dipped 10 times in between drying in oven at 150°C for 10 min. The proper calcination temperature will be investigated.

3.3 Sample characterisation

Characterisation is used as validation for ZnO present on the glass. It is executed through XRD and SEM. Further characterisation will be done by analysing results from photocatalytic activity, calcination temperatures etc.

3.4 Calcination temperature

The proper calcination temperature for thermal treatment is investigated with a furnace. Samples are prepared and treated in various temperatures (450-600°C) and is tested in the photocatalytic test. All samples have in common that the temperature ramp is 2°C/min and the holding time is 120 minutes before cooling to room temperature. The effect of the calcination temperature will be examined in the photocatalytic test.

3.5 Photocatalytic test

The photocatalytic test is conducted under same conditions each time as illustrated on the picture below.

Figure 13: Experiment setup in the light. All experiments takes place in the dark

The temperature is ambient at all times, and magentic stirring is applied to ensure a homogenous solution and exposion to the photocatalysis. The setup is kept dark when running an experiment.

The UV-VIS light is supplied by 3UV Series Handheld Lamps (3*8 watts) by UVP, and samples are only taken when the UV-light is turned of to ensure no damage to eyes and skin (UVP, 2016).

The control experiments used a UV-VIS light of 365 nm and sample is taken every 15 minute. The total volume is in the range of 150-200 mL which is appr. 2 cm in height.The testing takes place over a period of 210 minutes and examines the catalytic activity.

The samples will primarily be examined with Genesys 10 uv scanning and occasionally UV-3100PC Spectriphotmeter (will be indicated in the text).

4 Result and discussion

Characterisation of thin films

The ZnO films have been characterised by XRD by examining two samples. One film layer has been used 5 times for degrading dyes and one has never been used. By examining these two samples, it should be possible to see if changes do occur to the structure after a certain amount of usage, leading to a possible decrease in catalytic efficiency.

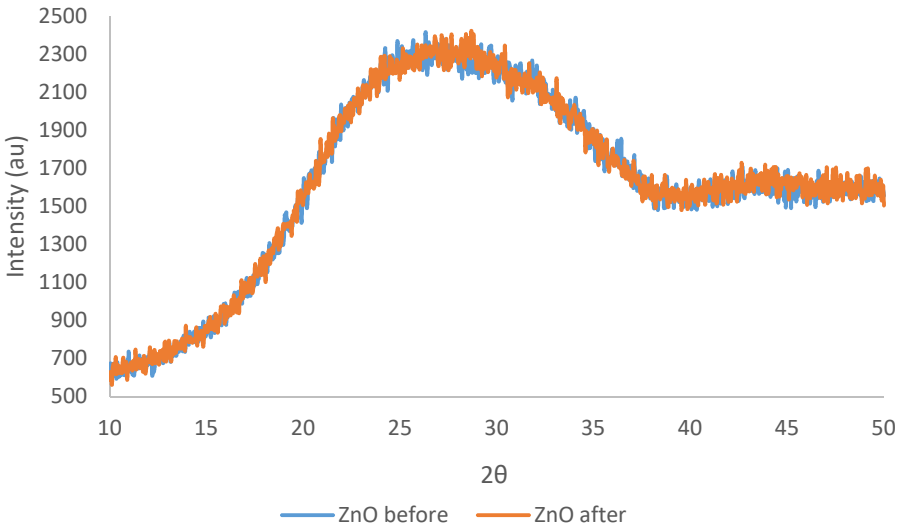

Figure 14: x-ray diffraction patterns for ZnO

As observable in Figure 14 there is no distinct peaks suggesting the orientation of the ZnO structure. It is known that between 30-40 2θ the (002) peak should have been present, see section 2.2.1. in the same range (100) and (101) should have been observable whereas (102) should be located around 45-50 2θ (Akhtar, et al., 2012). From the lack of distinct peaks and the curvature of the results it can be concluded that the ZnO films are amorph and thus must be analysed using a different method, such as electron microscope diffraction.

Both amorph and polycrystalline thin films possess no directionality or axis on a macroscopic plane, but there are some suggestions that if an amorphous state (liquid phase) is a random dense packing of atoms or microcrystallites. It is known that the growth of amorphous and polycrystalline thin films is independent of the substrate assuming there is no substrate-film interaction, and that and amorphous materials can be transformed to a polycrystalline state but the reverse is not possible (Mattes, 1980).

It is however well known, that glass is an amorphous structure thus does not have a regular crystal lattice, by avoiding crystallisation (Ojovan & Lee, 2010). This allows the random orientation of the ZnO nanostructure, even if it is not observable by method of XRD.

The films were analysed by SEM (Scaning Electron Microscopy) and it became apparent that the ZnO formed clusters. This is observable in Figure 15:

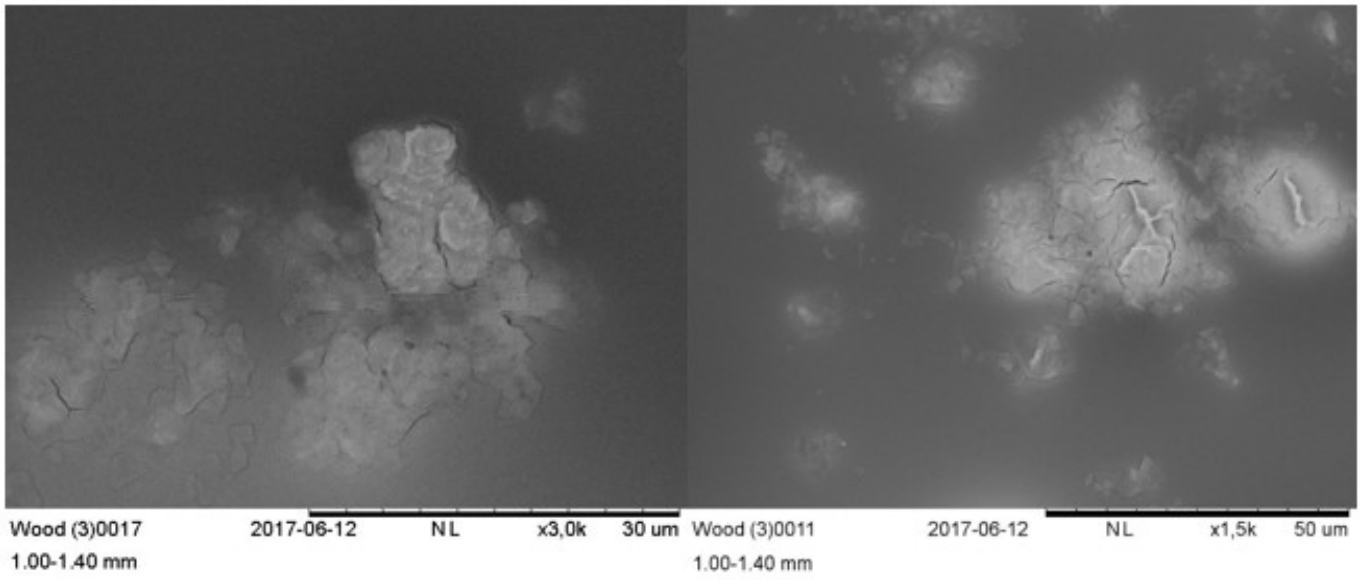

Figure 15: SEM images of unused ZnO film layer at 1500x (l) and 3000x (r)

It is also apparent, that at a magnification of 15000x/3000x it is not possibl to see any true nanostructure of ZnO (nanorods, wires etc), but it is more of irregular particles as observed by (Li & Haneda, 2003) when using spray pyrolýsis. Even though clusters have formed on the surface, and is thus not a true homogenous surface catalysis, it is still possible to examine surface-dependend behaviour, since it can be assumed that all film layers follow the same behavior, and the statistic variation is small. Furthermore, it can be seen that while the structure is irregular particles, it is not possible to see any specific orientation of the nanostructure, thus it is reaffirmed that glass surfaces gives an random orientation of the ZnO nanoparticles.

Glass plates- random orientation

The calciniation temerature has been investigated as a function of the rate law constant, k. This was held up against a control test, run under same conditions. This is observable in Figure 16.

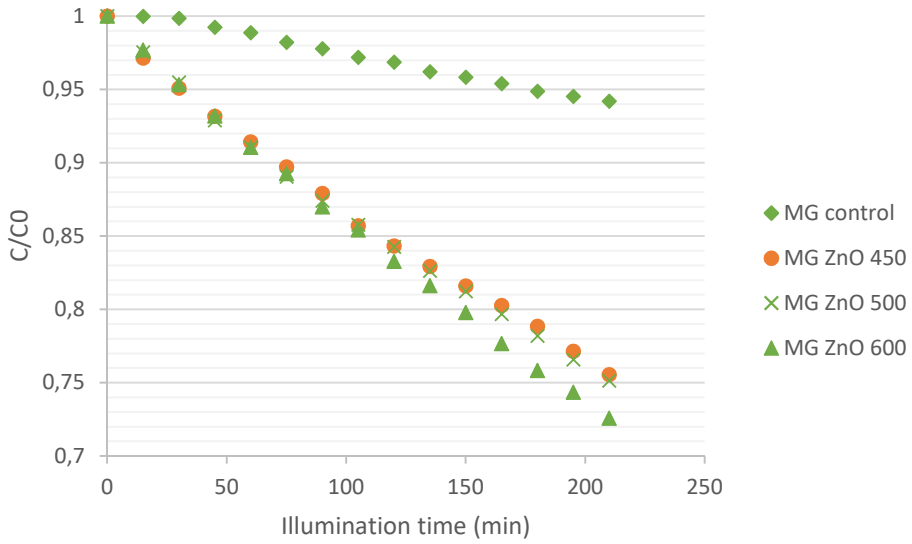

Figure 16: MG calcination temperatures dependence

It becomes apparent that ZnO has an effect on MG solution, and that there is a slight tendency to temperature dependence, however when observing the kinetics the variation is so small, that it is negible. This is shown in Table 3 below.

Table 3: rate law constant for MG solution

Sample name	Rate constant	Half life
Control MG	0.0003 min^{-1}	2311 min
MG ZnO 450°C	0.0013 min^{-}	533 min
MG ZnO 500°C	0.0013 min^{-}	533 min
MG ZnO 600°C	0.0015 min^{-}	462 min

It is known that it follows a first order reaction kinetics, since when $\ln(C/C_0)$ gives a straight line with the rate constant as the slope. This is also expressed in several research papers for various dyes as an pseudo-first order reaction kinetics (Stambolova, et al., 2014), (Balcha, et al., 2016).

From these experiments, two things can be concluded (1) ZnO has a positive effect on color degradation of MG (25% vs. 5.8%) with random ZnO orientation and (2) While there is a slight temperature dependence the difference is slight enough, that in this case, it is neglible and that 450°C is the best temperature since it uses less energy. It was investigated how much the rate constant would change as a function of initial concentration, and it was found that if the initial concentration applied in ZnO 600°C was adjusted downwards with approximately 1.5 ppm the rate law constant increased to 0.0023 min^{-1}, which is only 0.0010 min^{-1} to (Stambolova, et al., 2014) ZnO film sample. With the increased rate constant the half lime decreased to 302 minutes compared to the 462 minutes previously.

For MB, the situation is quite different, due to its insensitivity to light at a neutral pH value.

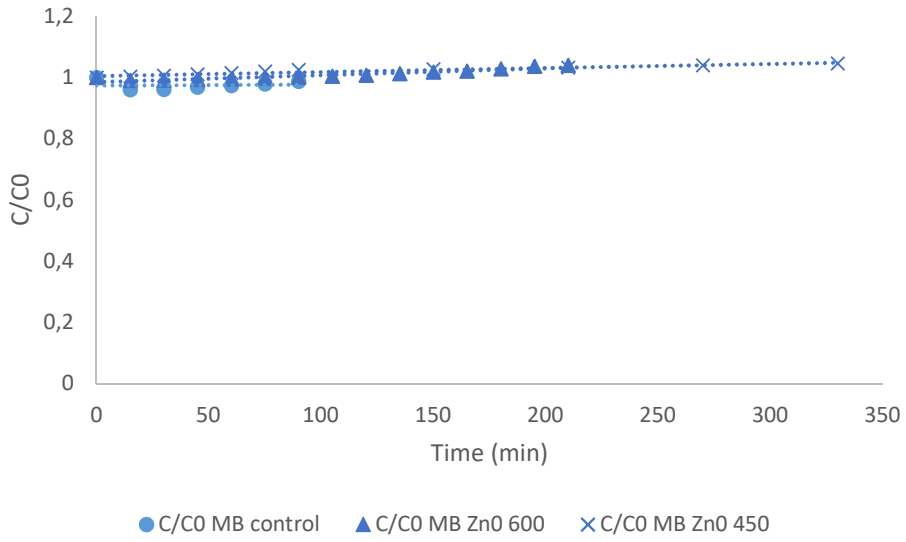

Figure 17: MB sensitivity to light

Figure 17 clearly indicates that with or without a catalyst, MB is not reduced to a colorless form or has reacted into a different carbohydrate. This may indicate that MB is quite sensitive to pH values, since all solutions is based upon MiliQ water, which has a neutral pH value (in theory, practical it is about pH=6). Thus, it is tested wether pH has an influence and how sensitive it is to it. It is known that in water (1% solution) that the pH is between 3-4.5 (pubchem, 2017) which is on the acid side, so if a teaspoon of caustic soda (about 4.5 g) is added and no exposure to light or catalyst the following trend emerges:

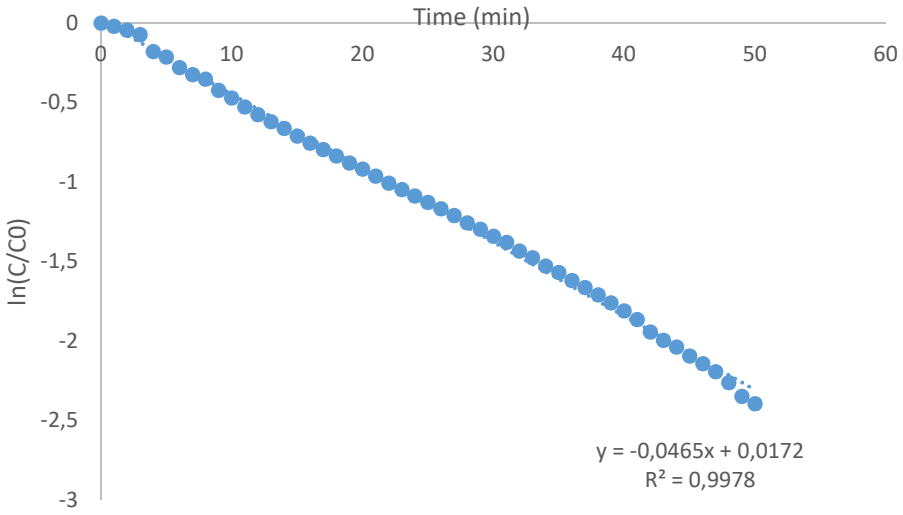

Figure 18: MB sensitivity to change in pH value

Figure 18 clearly indicates that MB is extremely sensitive to changes in pH and do transform/decolorises as a 1.order kinetic reaction, even with no exposure to light. The rate constant is extremely high (0.0465 min^{-1} when compared to MG's rate constant) and has a decolorisation of 91% after 50 minutes. Plus some gasses have been created (due to odor), which suggest that the decolorisation is irreversible. This suggest, that if the waste water is basic, then MB will be transformed even without the presence of a catalyst. The

decolorisation could not be seen in the solution, since it retained its dark blue color, however when left over few days, the color is transformed to purple with a new maximum absorbance, which suggest that MB has reacted with NaOH and is thus a new purple product, most likely resazurin (analysed by UV with a λ_{max} at 598 nm, consistent with theory). Thus, pH value of MB and MG has been examined and found to be exactly the same (pH=5), 5 and since the increase in pH value indicated a new dye has been created, perhaps a decrease in pH value will produce better results as shown by (Mohabansi, et al., 2011).

Unfortunately even with the dye concentration as used in (Mohabansi, et al., 2011) it has been impossible to degrade MB with only ZnO as a catalyst. This is most likely due to either the photocatalyst load or the nanostructure and size of crystallite size.The cause is not that ZnO generally is unable to degrade MB since (Mohabansi, et al., 2011) and (Balcha, et al., 2016) has shown it is possible. Since at the current time of the experimental work, the nanostructure and its defects/crystallite size has not been examined, the photocatalytic load will be examined first by applying all three ZnO films (ZnO 450, ZnO 500, ZnO 600) to a 5 ppm solution. This however proved to be fruitless see Figure 17, and thus it must be assumed that it is the nanostructure which is at play. It is known from (Balcha, et al., 2016)that a hexagonal wurtzite structure (nanoparticles) with an average crystallite size of 28-30 nm is successful in degrading more than 80 % MB over a course of 200 minutes. They also concluded that photocatalytic load, initial dye concentration and manufacture method of ZnO all influences the degradation. To ensure it is the nanostructure, and not inactive photocatalyst a MG photocatalytic test was run with a positive result, confirming that while the photocatalyst is active it is not capable of degrading MB. MB will not be investigated further. However the relationship between catalystic area and rate constant has been investigated for MG at 3.5 ppm, and the following graph explains the correlation.

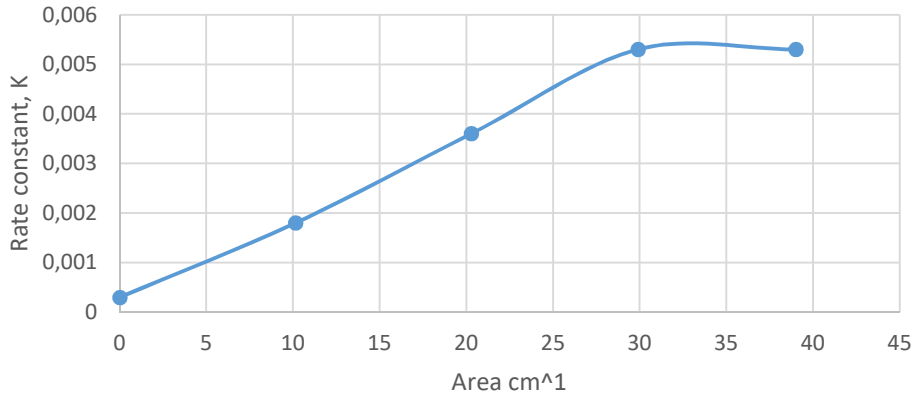

Figure 19: Correlation between rate constant and area for MG

As observable in Figure 19 there is a linear relationship between catalysis area and rate constant up to a certain degree which follows the function of:

$y = 0{,}0002x + 0{,}0002$

which is valid for $\{0 \geq x \leq 29.9\}$. Furthermore according to the linear function it intersept y-axis at 0.002 min^{-1} which is pretty close to the experimental value of 0.003 min^{-1} when no catalyst is present. It also validates that the calcination temperature has no influence since all the small varieties in the rate constant has been verified to be small differences in the exposed surface area. With the optimal surface area of 29.9 cm^2 the rate constant is 0.0053 min^{-1} which is 60% improvement compared to (Stambolova, et al., 2014) if initial

concentration dependence is neglected. (Gnanaprakasam, et al., 2016) studied the effect the amount of doped ZnO nanoparticles could have and found the following in Figure 20:

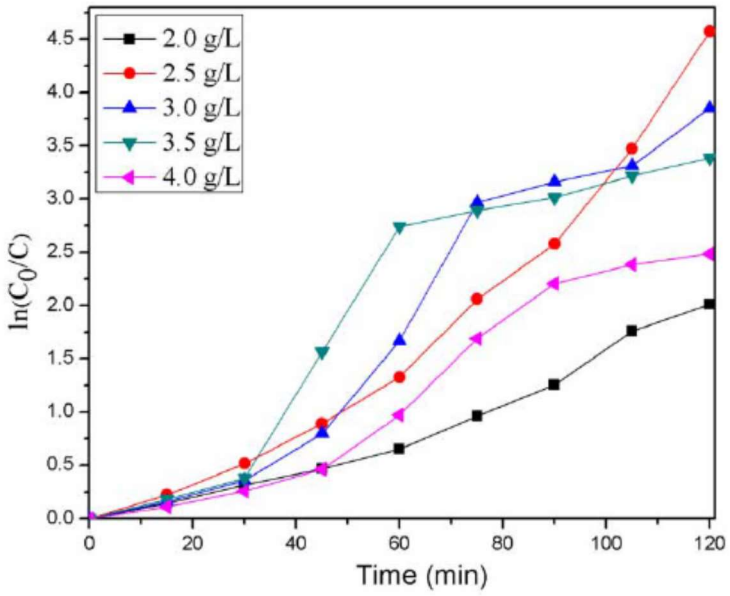

Figure 20: Effect of 2% Ag doped ZnO of 10 ppm BG (Gnanaprakasam, et al., 2016)

Where there is no proper linear relationship between catalysis amount and degradation of BG (brilliant green), due to the fact that when the catalytic load is increased more than 0.35 g/L the rate constant *k*, decreases. This is due to that when the catalytic load is increased, the number of available active sites for adsorption increases and so do oxidizing radicals (increase degradation). However when the optimum level is exceeded the turbidity of the dye solution increases which reduce light penetration thus unavailability of photons for degradation, see section 2.2, on the surface of the catalyst, leading to a reduction in photocatalytic degradation. Similar conclusion may be drawn for MG, but it is impossible to further analyse the phenomena due to limitations in the experimental set-up i.e. not enough space for more film.

Hypothesis: since the structure between MG and MB is so different the ZnO photocatalytic film layer may only work for the tri-phenyl categories of paint, see section 2.1.

There is only a small structural variation between BG and MG, where the strcture of BG is shown in Figure 21:

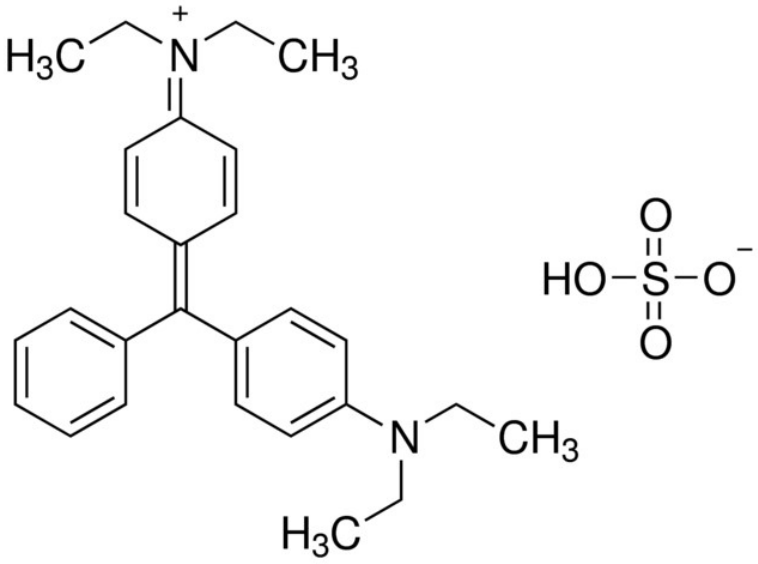

Figure 21: Structure of BG (Sigma-Aldrich, 2017)

When compared to Figure 3 (b) the major difference is the length of the carbon chain attached to nitrogen, and that there is a small amount of sulphur present.

It has been noted that BG is a little bit unstable in UV radiation with the absence of TiO_2 (similar photocatalyst to ZnO), but it is possible to degrade it at 365 nm in a TiO_2 dispersion (Chen, et al., 2008). This makes it possible for ZnO to accomplish the same since it is in some cases possible to exchange TiO_2 for ZnO. This was validated by (Gnanaprakasam, et al., 2016) who applied doped and undoped ZnO nanoparticles to a 10 ppm BG solution under UV irradiation and observed a pseudo-first order kinetics (degradation of BG).

By following the same initial conditions as for area dependence of MG (optimal catalytic area for MG used) it was possible to achieve a rate constant of 0.0076 min^{-1}. However it must be noted that the first few measurements (0-30 minutes) were excluded due to instability of the absorbance. The pseudo-first order linear relationship was determined to be between 90-210 minutes, as observable in Figure 22:

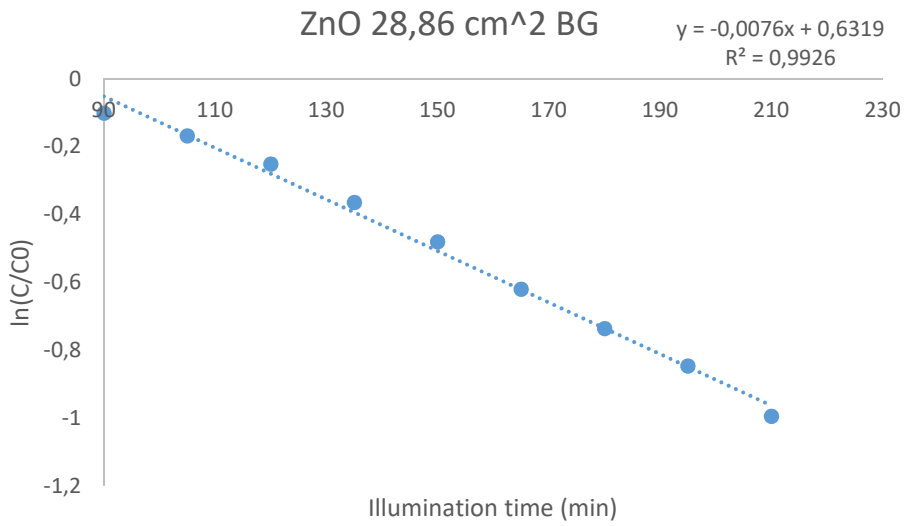

Figure 22: pseudo-first order kinetics for BG at 3.5 ppm

When comparing the rate constants between MG and BG it becomes apparent that while the dyes are very similar in structure the degradation occurs more rapidly for BG, since the rate constant has increased by almost 40 %.

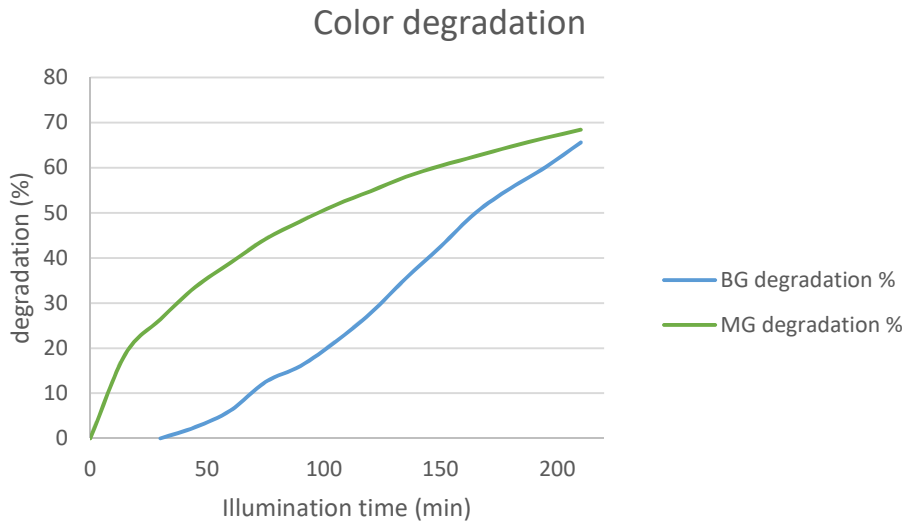

Figure 23: Color degradation for MG and BG

When comparing BG and MG color degradation in Figure 23 it becomes apparent that they follow two different trends. MG degradation appears to be exponential whereas BG degradation is more linear. It was also noted that for the first hour or so BG was unstable in the water, causing an increase in the absorbance (hyperchromic effect**)** which was likely caused due to inhomogenity in the solution or the reaction pathway for BG degradation (similar to that of DNA denaturation) (Kumar, 2006), (Chemistry-Dictionary.com , 2015).

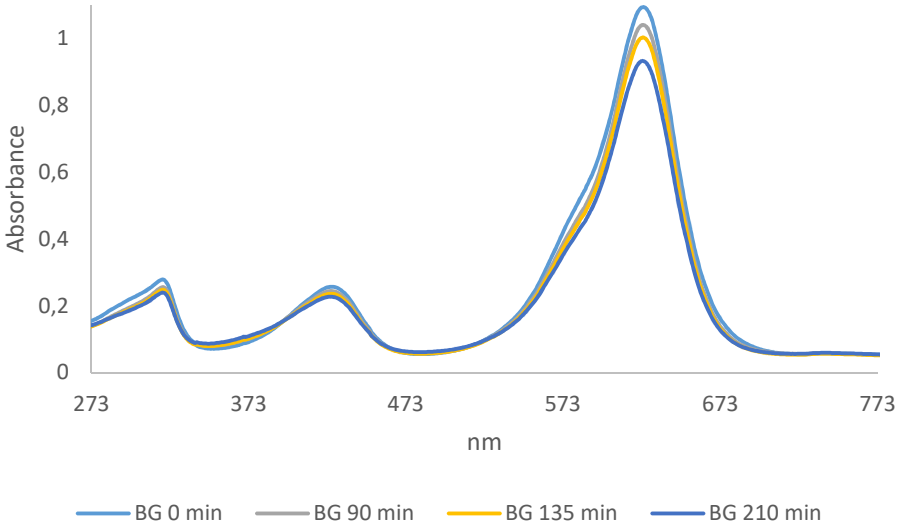

Figure 24: BG degradation measured on UV-3100 PC Spectrophotometer

Figure 24 illustrates the degradation of BG and shows the three important peaks for BG. It is apparent that while the intensity of the absorbance is dwindling, there is no shift in the wavelength of the λ_{max} which confirms that while BG has a tendency to increase slightly in concentration during the initial 60-90 minutes, it is not due to a shift for λ_{max}.. It can however be noted that at appr. 319 nm there is an absorbance most likely caused by an aromatic ring, which is decreasing indicating that the aromatic ring is being opened during the degradation.

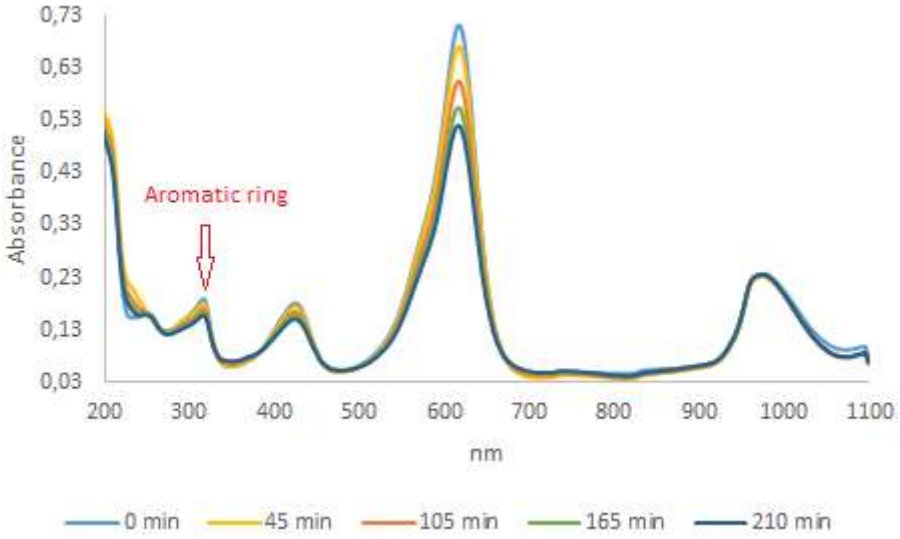

Figure 25: MG degradation measured on UV-3100 PC Spectrophotometer

The same conclusions can be drawn for MG degradation as shown in Figure 25 where all absorbance peaks decrease steadily, all indicating a breakdown of MG into new compounds, which are hopefully less toxic to the environment.

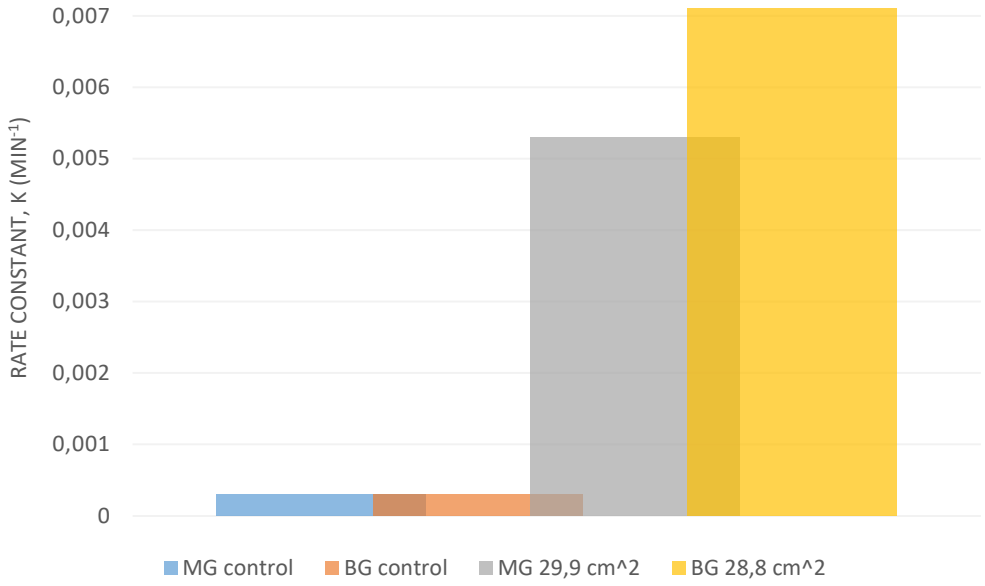

Figure 26: Comparison of different rate constants for MG and BG

Figure 26 indicates that when both initial concentration and surface area of the catalysts are similar for both MG and BG there is a distinct difference between catalytic activity. Since the slight structural difference is the only parameter influenced it is apparent that the molecular structure has a distinct influence on catalytic activity, and thus it can be assumed that the molecular structure of MB did influence the inability of color degradation. It can also be noted the major influence a photocatalyst has on the colored water. That while it is possible for a 'natural' degradation the catalyst has a clear influence on finding a faster reaction pathway. It must be notes that the results do not display the average steps in the catalytic circle but rather the slowest, meaning that some steps may be faster than what the results shows.

4.1 Limitations in methodology

There is a significant limitation in the dip coating manufacture, which is evaporation of water. While the evaporation is an important factor to make the film adhesive to the surface, thus the low speed, it also limits the production of film layers. This is due to the open container system used in dipcoating, causing water to evaporate from the container and the slow speed (1 mm/min) indictes, that the 10 dips necessary takes longer than 10 hours. This causes a significant evaporation from the container, causing zink acetate to be precipitated in the solution. This leads to uneven layers on the surface, thus influencing the capabilities of the photocatalyst.

The evaporation of water from the solution can be eliminated by isolate the system in a dome and use water steam (exchange air with water vapors) under the dome to ensure no evaporation of water. It may, however influence the adhesion to the glass surface, but this has not been investigated in this report.

Another limitation in the set-up also correlates to the ZnO films, just in another way. This limitations is caused by the limited area at the bottom of the set-up (the container for the dye), which limits the test of area dependence since only four pieces of microscope glass can fit the bottom without laying on top of each other or hitting the magnetic stirrer.

5 Conclusion

It is possible to achieve ZnO films on a glass substrate using a dipcoater method with a speed of 1 mm/min to achieve a thin layer which is amorphous. It is possible to achieve a proper calcination at lower temperatures (450°C) leading to a decreased energy usage for the process, and it was discovered that there is a relation between surface area of the catalyst and activity expressed as rate constant, *k* expressed in a first order reaction kinetics.

The specific orientations and which one ZnO is inclined towards is unknown due to the amorphous state of the ZnO films. It must be supplemented with other methods wxhich examines morphology such as FE-SEM or a cross-section examination by usage of SEM. From SEM pictures it was possible to conclude that ZnO forms small clusters, where it is possible to see that the orientation appears random, and that the nanoparticles has a tendency to lay on top of each other, which is most likely caused by the repeated dipping.

It was not possible to degrade MB without any usage of pH changing sources, with this type of ZnO, the study of MB in this paper is limited.

It is possible to degrade MG and BG, which are similar in structure since both have a tri-phenyl as the backbone of the dye. It is however notable that with the same catalytic load and approximately same initial concentration the rate constant has a 40% variation and that the color degradation pattern is not similar (exponential vs. linear).

When comparing MG and BG rate constants on runs with and without catalysis (optimum surface area) it is an improvement of 94.3 % and 95.8 %, respectively. It demonstrates that the presence of a catalyst will decrease the lifespan of an aqueous dye in wastewater.

It is however unknown what the dyes are degraded to exactly, with the exception of water and a gas, so it is not possible to conclude if the resulting products are less damaging to the environment than the dyes themselves.

6 References

Akhtar, J. et al., 2012. Zinc oxide nanoparticles selectively induce apoptosis in human cancer cells through reactive oxygen species. *Int. J. Nanomedicine* , 21 February, p. 845—857 .

Balcha, A., Yadav, O. P. & Dey, T., 2016. Photocatalytic degradation of methylene blue dye by zinc oxide nanoparticles obtained from precipitation and sol-gel methods. *Environ Sci Pollut Res*, 4 October, p. 25485–25493.

Callister, W. D. & Rethwisch, D. G., 2011. *Material Science and Engineering.* 8. ed. Asia: John Wiley and Sons.

Cennens, J., Schoonheydt & A., 1988. VISIBLE SPECTROSCOPY OF METHYLENE BLUE ON HECTORITE,LAPONITE B, AND BARASYM IN AQUEOUS SUSPENSION. *Clays and Clay Minerals,*, pp. Vol. 36, No. 3, 214-224.

chemicalbook, 2016. *chemicalbook.* [Online]
Available at: http://www.chemicalbook.com/ChemicalProductProperty_EN_CB3748860.htm
[Accessed 14 March 2017].

Chemistry-Dictionary.com , 2015. *Chemistry Dictionary.* [Online]
Available at: http://www.chemistry-dictionary.com/definition/hyperchromic+effect.php
[Accessed 04 07 2017].

Chen, C.-C.et al., 2008. Photocatalyzed N-de-ethylation and degradation of Brilliant Green in TiO2 dispersions under UV irradiation. *Desalination*, pp. 89-100.

Chequer, F. M. D. et al., 2013. Chapter 6, Textile Dyes: Dyeing Process and Environmental Impact. In: M. Gunay, ed. *Eco-Friendly Textile Dyeing and Finishing.* s.l.:INTECH, p. Chapter 6.

Company, D. C., 2006. *CHEMICAL EXPOSURE INDEX.* s.l.:Dow Chemical Company.

Gnanaprakasam, A., Sivakumar, V. & Thirumarimurugan, M., 2016. A study on Cu and Ag doped ZnO nanoparticles for the photocatalytic degradation of brilliant green dye: synthesis and characterization. *Water Science & Technology*, 28 June, pp. 1426-1435.

Jo, Wan-Kuen, T. & J., R., 2014. Recent developments in photocatalytic dye degradation upon irradiation with energy-efficient light emitting diodes. *Chinese Journal of Catalysis*, 20 November, pp. 1781-1792.

Khan, M. M., Adil, S. F. & Al-Mayouf, A., 2015. Metal oxides as photocatalysts. *Journal of Saudi Chemical Society*, 27 April, pp. 462-464.

Khezami, L., Taha, K. K., Ghiloufi, I. & El Mir, L., 2016. Adsorption and photocatalytic degradation of malachite green by vanadium doped zinc oxide nanoparticles. *Water Science and Technology*.

Kołodziejczak-Radzimska, A. & Jesionowski, T., 2014. Zinc Oxide—From Synthesis to Application: A Review. *Materials*, 9 April, pp. Vol 7, 2833-2881.

Krechetnikova, R. & Homsy, G., 2005. Dip coating in the presence of a substrate-liquid interaction potential. *PHYSICS OF FLUIDS*, 19 October, p. Vol. 17.

Kumar, S., 2006. *Spectroscopy of Organic Compounds,* s.l.: Guru Nanak Dev University.

Lemlikchi, S. et al., 2010. Study of structural and optical properties of ZnO films grown by pulsed laser deposition. *Applied Surface Science*, p. 5650–5655.

Li, D. & Haneda, H., 2003. Morphologies of zinc oxide particles and their effects on photocatalysis. *Chemosphere*, pp. 51, 129–137.

Li, D. & Haneda, H., 2003. Morphologies of zinc oxide particles and theireffects on photocatalysis. *Chemospher*, pp. vol 51, 129-137.

Ltd., W. L., 2011. *Methods of chemical synthesis and purification of diaminophenothiazinium compounds including methylthioninium chloride (MTC).* AT BE BG CH CY CZ DE DK EE ES FI FR GB GR HU IE IS IT LI LT LU LV MC NL PL PT RO SE SI SK TR , Patent No. EP 2 322 517 A1.

Lu, C. et al., 2009. Degradation efficiencies and mechanisms of the ZnO-mediated photocatalytic degradation of Basic Blue 11 under visible light irradiation. *Journal of Molecular Catalysis A: Chemical*, 17 June, p. 159–165.

Mattes, B. L., 1980. Growth and structure of amorphous and polycrystalline thin films. In: L. L. Kazmerski, ed. *Polycrystalline and amorphous thin films and devices.* New York: Academic Press, pp. 1-14.

Merck, 2017. *merckmilipore.dk.* [Online]
Available at: http://www.merckmillipore.com/DK/en/product/Polietilenglicole-200,MDA_CHEM-807483?ReferrerURL=https%3A%2F%2Fwww.google.dk%2F
[Accessed 15 March 2017].

Mohabansi, N., Patil, V. & Yenkie, N., 2011. A COMPARATIVE STUDY ON PHOTO DEGRADATION OF METHYLENE BLUE DYE EFFLUENT BY ADVANCED OXIDATION PROCESS BY USING TiO2/ZnO PHOTOCATALYST. *RASAYAN J. Chem*, pp. 814-819.

Mortimer, C. E., 1975. Grinard reagents. In: J. C. Carey, ed. *Chemistry, six edition.* Belmont: Wadsworth Publishing Company, pp. 813-814.

Nehru, L., Umadevi, M. & Sanjeeviraja, C., 2012. Studies on Structural, Optical and Electrical Properties of ZnO Thin Films Prepared by the Spray Pyrolysis Method. *International Journal of Materials Engineering*, pp. 12-17.

Ojovan, M. I. & Lee, W. (. E., 2010. Connectivity and glass transition in disordered oxide systems. *Journal of Non-Crystalline Solids*, 9 June, p. 2534–2540.

Pro-Lab Diagnostics, 2016. *Safety Data Sheet Malachite Green,* Wirral : Pro-Lab Diagnostics.

pubchem, 2017. *pubchem.* [Online]
Available at:
https://pubchem.ncbi.nlm.nih.gov/compound/Methylene_Blue_trihydrate#section=Absorption-Distribution-and-Excretion
[Accessed 14 March 2017].

pubchem, 2017. *pubchem.* [Online]
Available at: https://pubchem.ncbi.nlm.nih.gov/compound/ethanol
[Accessed 14 March 2017].

pubchem, 2017. *pubchem.* [Online]
Available at: https://pubchem.ncbi.nlm.nih.gov/compound/acetone#section=Density
[Senest hentet eller vist den 14 March 2017].

pubchem, 2017. *pubchem.* [Online]
Available at: https://pubchem.ncbi.nlm.nih.gov/compound/ethylene_glycol#section=Fire-Fighting
[Accessed 15 March 2017].

Rankin, D. W., Mitzel, N. W. & Morrison, C. A., 2013. 10. Diffraction Methods. In: D. Atwood, B. Crabtree, G. Meyer & D. Wollins, eds. *Structural methods in molecular inorganic chemistry.* Malaysia: Wiley, pp. 304-308.

Rankin, D. W., Mitzel, N. W. & Morrison, C. A., 2013. *Structural methods in molecular inorganic chemistry.* 1. ed. s.l.:John Wiley and Sons.

Raval, N. P., Shah, P. U. & Shah, N. K., 2016. Malachite green ‘‘a cationic dye’’ and its removal from aqueous solution by adsorption. *Applied Water Science*, 18 December, pp. 1-39.

Rothenberg, G., 2008. *Catalysis Concenpt and Green Applications.* Germany: Wiley-VCH.

Rothenberg, G., 2008. *Catalysis, Concepts and Green Applications.* Weinheim: Wiley-VCH.

Sanzaro, S. et al., 2016. Multi-Scale-Porosity TiO2 scaffolds grown by innovative sputtering methods for high throughput hybrid photovoltaics. *Scientific Reports*, 21 December, pp. Vol 6, 1-15.

Saravanan, R., Guptar, V. K., Narayanan, V. & Stephen, A., 2013. Comparative study on photocatalytic activity of ZnO prepared by different methods. *Journal of Molecular Liquids*, 19 March, pp. 133-141.

Sartape, A. S. et al., 2014. Removal of malachite green dye from aqueous solution with adsorption technique using Limonia acidissima (wood apple) shell as low cost adsorbent. *Arabian Journal of Chemistry*, pp. 1-10.

scbt, 2017. *scbt.* [Online]
Available at: https://www.scbt.com/scbt/product/zinc-acetate-557-34-6
[Accessed 14 march 2017].

scbt, 2017. *scbt.* [Online]
Available at: https://www.scbt.com/scbt/product/malachite-green-oxalate-salt-2437-29-8
[Accessed 14 March 2017].

Schwartz, L. & White, L., 1994. *Modelling of the dip-coating process,* s.l.: Mathematics in Industry.

Sigma Aldrich, 2017. *Sigmaaldrich.dk.* [Online]
Available at: http://www.sigmaaldrich.com/catalog/product/sial/81150?lang=en&region=DK
[Accessed 09 02 2017].

sigma-aldrich, 2017. *sigma-aldrich.* [Online]
Available at: http://www.sigmaaldrich.com/Graphics/COfAInfo/SigmaSAPQM/SPEC/M9/M9015/M9015-BULK SIGMA .pdf
[Accessed 28 January 2017].

Sigma-Aldrich, 2017. *Sigma-Aldrich.* [Online]
Available at:

http://www.sigmaaldrich.com/catalog/substance/brilliantgreen4826363303411?lang=en&region=DK [Accessed 10 June 2017].

Silverstein, R., Bassler, G. C. & Morril, T. C., 1991. *Spectrometic identification of organic compounds.* 5. ed. s.l.:John Wiley and Sons.

Sing, M. et al., 2014. Bio-sorbable, liquid electrolyte gated thin-film transistor based on a solution-processed zinc oxide layer. *Faraday Discuss.*, 9 May, pp. 174, 383–398.

Stambolova, I., Kaneva, N., Shipochka, M. & Vassilev, S., 2014. Effect of titanium dopant on the surface features and on the photocatalytic characteristics of ZnO films. *Materials Science in Semiconductor Processing*, pp. 244-250.

Taabouche, A. et al., 2013. Effect of Substrates on the Properties of ZnO Thin Films Grown by Pulsed Laser Deposition. *Advances in Materials Physics and Chemistry,*, pp. 209-213.

U.S. Department of Health and Human Services, 1994. *Toxicological Profile For Acetone,* Atlanta, Georgia: Agency for Toxic Substances and Disease Registry.

UVP, 2016. *3UV Series Handheld Lamps Operating Instructions.* Upland, CA: UVP, an Analytik Jena Company.

VWR, 2016. *SAFETY DATA SHEET,* Solon, Ohio: VWR International.

Wake Fores University, Chemistry 223L, 2017. *wfu.edu.* [Online]
Available at: https://users.wfu.edu/~kingag/223L/procedures-handouts/12-grignard.pdf
[Accessed 03 May 2017].

William Reusch, 2017. *chemistry.msu.edu.* [Online]
Available at: https://www2.chemistry.msu.edu/faculty/reusch/virttxtjml/spectrpy/uv-vis/spectrum.htm
[Accessed 19 April 2017].

Yuan, L. et al., 2014. Temperature-dependent growth mechanism and microstructure of ZnO nanostructures grown from the thermal oxidation of zinc. *Journal of crystal growth*, 15 March, pp. 101-108.

7 Appendices

7.1 Appendix 1: standard curves

Two standard series, methylene blue trihydrate(MB) and malachite green oxalate(MG), is based on 40 ppm solutions. All water mentioned in this section is equal to MiliQ water, due to the fact that pH can influence later results (different types of water equalt to different pH values. All samples has been measured on genesys 10uv scanning from Thermo scientific.

Table 4: Dilution table to achieve 40 ppm

Malachite green oxalate		**methylene blue trihydrate**
M (g/mol)	463.5	373.896
m (g)	0.04056	0.04061
V (mL)	1000	1000
C (mg/mL)	0.04056	0.04061
ppm	40.56	40.61

As it can be observed from the table 0,04 g of the dyes has been weigthed out and diluted up to 1000 mL to achieve 40 ppm. This gives the solutions a dark color (blue with a green tint(MG) and dark blue(MB)). They will be diluted further during the spectroscopic measurements (UV) to achieve a standard curve used to calculate the concentrations of the dyes during degradation.

From the standard series linear function it is possible to express concentration (ppm) as:

$$n = \frac{absorbance - \beta}{\alpha}$$

Where absorbance is the measured absorbance to its belonging wavelength(where it peaks). It is also possible to use Lambert-Beers law and find the specific absorbance coefficient, ε.

The spectophotometry couldn't measure anything over 3 in absorbance thus, the first measureable concentration was 10 ppm. It had a maximum at 618 nm, so all samples were measured at that wavelenght.

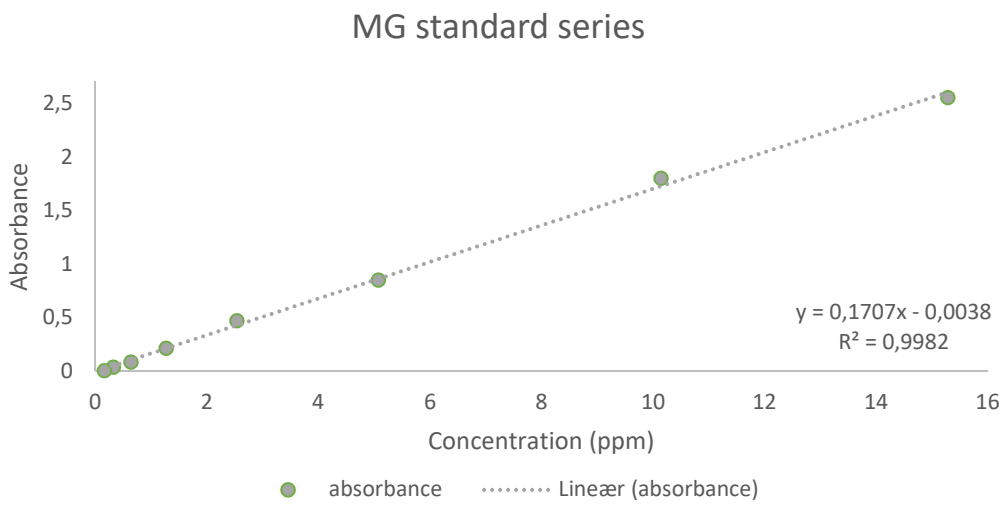

Figure 27: MG standard series

As it can be observed it is an acceptable fit, considering uncertanities when using pipettes.

The 10 mL pipette used to measure MG has an uncertanity of +-0.075 mL and it was difficult to get the last few drops out.

The 5 mL pipette used to measure MiliQ water has an uncertanity of +-0.03 mL and it was difficult to get the last few drops out.

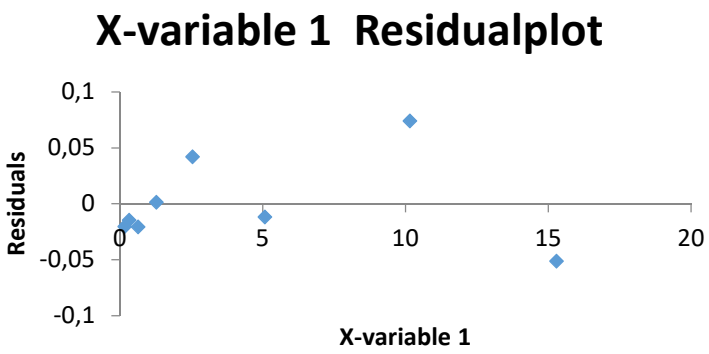

Figure 28: Residual plot for MG standard series

As it is apparent from Figure 28 it is confirmed that MG standard curve is linear.

MB:

According to (Cennens, et al., 1988) MB absorb at 664 nm in aqueous solutions, which is consitent with the measured maximum at 664 nm.

There are some uncertanity when using the pipettes. It is difficult to get the last few drops out, especially true for the water pipette.

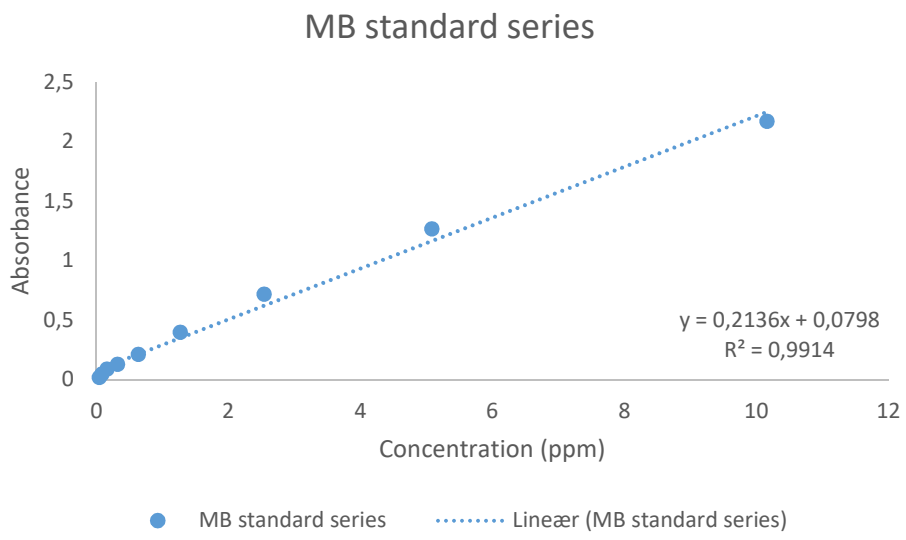

Figure 29: MB standard series

The fit is decent however it is noticeable that the last few dilutions are not a straight line. This may have something to do with the uncertainty of the pipetting, since it increases for each dilution.

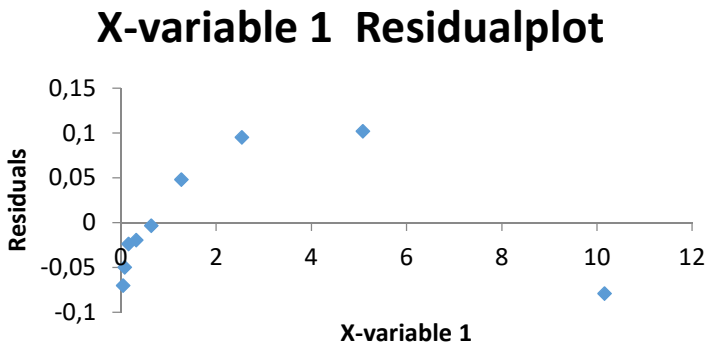

Figure 30: Residual plot for MB standard curve

Figure 30 demonstrates that MB standard curve is indeed linear.

BG:

BG has an absorbance around 630 nm according to (Gnanaprakasam, et al., 2016), and for the applied equipment in this report, the absorbance was at 624 nm. The solution of BG was made from following measurements:

Table 5: Dilution table to chieve 40 ppm BG

M (g/mol)	
m (g)	0.04109
V (mL)	1000
mg/mL	0.04109
ppm	41.09

The standard curve for BG was achieved to be:

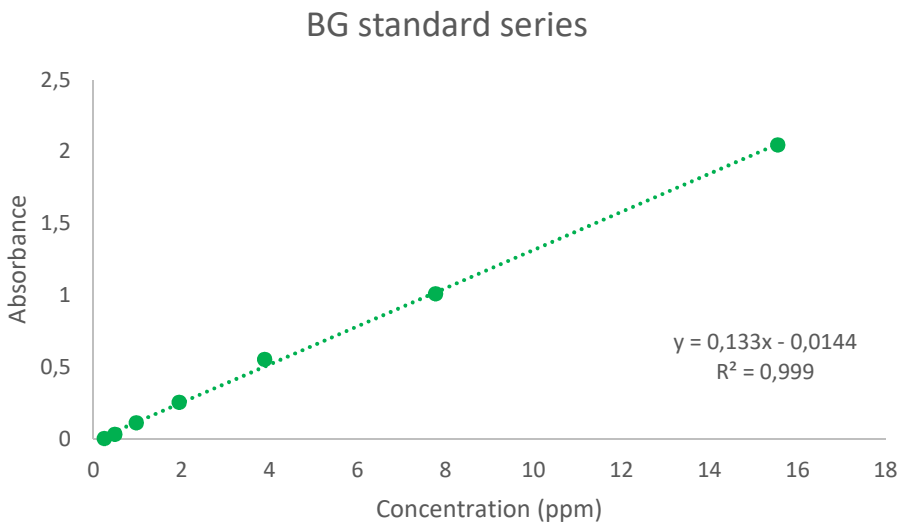

Figure 31: Standard curve for BG

With the belonging residual plot, to prove linearity:

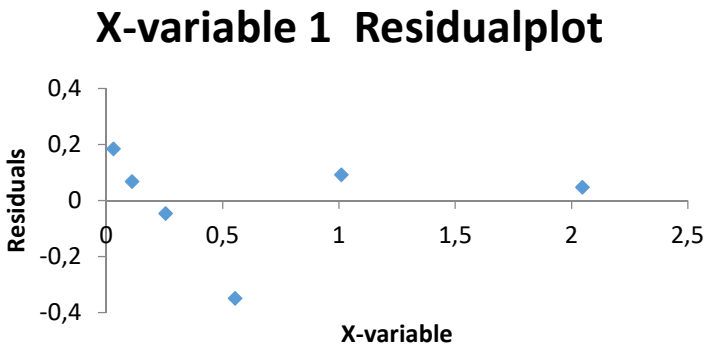

Figure 32: Residual plot for BG standard curve

7.2 Appendix 2: Determination of Zn^{2+} concentration for proper film making

The concentration of the aqueous zinc acetate has to be determined through experiments due to lack of information of proper concentration to get a good film layer on the glass.

Between each measurement/control of film layer the glas plate is cleaned with ethanol and acetone to ensure it is not covered in grease and other dirt which wil influence the film layer.

The glass plate is dipped into the solution at a speed of 20 mm/min to ensure an even layer. The temperature of the solution is ambient.

It was discovered that the best possible concentration was near the saturation point (430 g/L) at a lower dipping speed of 1 mm/min. Near saturation point, does give some issues, since evaporation of water leads to precipitation.

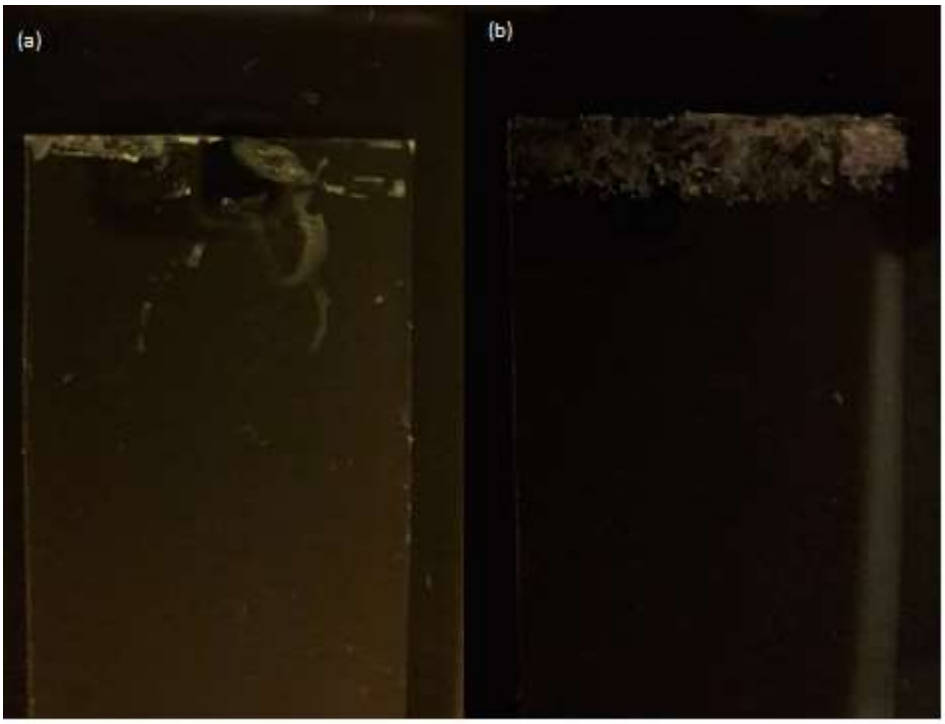

Figure 33: (a) Zn-film at C=1.4 M leaves an inhomogenous film layer (b) Zn-fil at C>2.3 M is inhomogenous but the solution was supersaturated, which means the concentration is too high

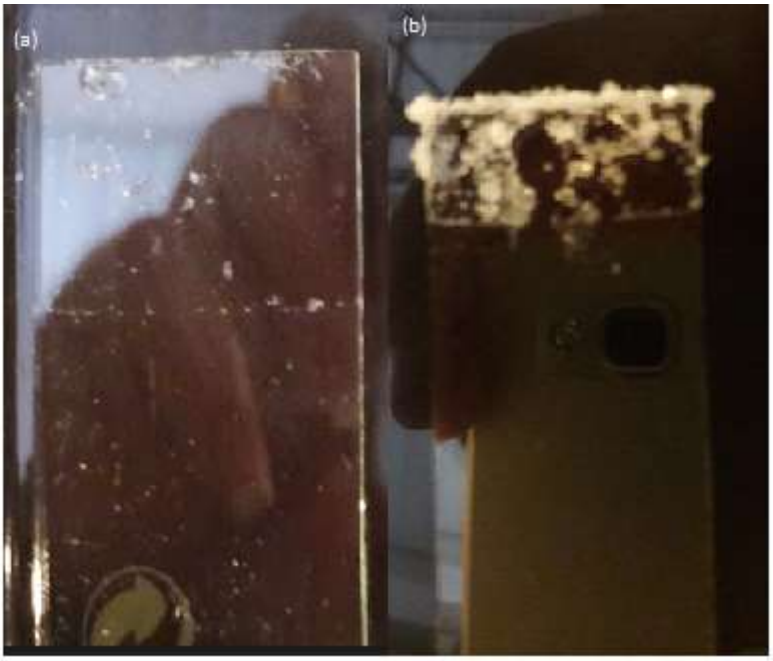

Figure 34: both samples were run at C=2.3 M (a) has a speed of 10 mm/min and (b) 1mm/min which suggest speed has a major influence on adhesion

However, adhesion is an issue, which is necessary to research to achieve a homogenous film layer.

Poly (ethylene glycol) is added to the solution, which should stick better to the glass surface. It is tested with a aq. Zinc acetate at 1.7 M. Different amounts of poly ethylene glycol were tested, and all it led to was precipitation of zink acetate and if foam was present it was possible to make a foam film layer on the glass. It indicated tha the concentration was too high (near saturation point), thus a reduction in concentration was necessary.

(Stambolova, et al., 2014) indicated that a lower concentration of zink acetate with 40 wt% of ethyl cellulose relative to the zink salt a film layer is possible. Similar concenpt was tested with a 0.8 M zinc acetate and various amounts of poly (ethylene glycol). It was discovered that with the presence of 19 mL poly(ethylene glycol) a very thin and homogenous film layer is produced with a dipping speed of 3 mm/min where the glass have been in the solution for a few minutes. The layer is too thin and transparrent so further layers is put on top, to get an even homogenous layer, 10 dips where needed, where the film layer was dried in-between each dip for 10 minutes at 150°C.

7.3 Appendix 3: CEI calculation for ethanol

CEI calculations have been completed by following the 6 steps given in (Company, 2006) under a few assumptions, such as ethanol is stored at ambient conditions and is only for a smaller scale-up of 100 L.

Table 6: CEI calculations for ethanol under assumption it is kept at ambient temperature and pressure

	Ethanol	Unit
Pg	101.325	kPa
Temp	25	Celcius
Normal BP	78.29	Celcius
Density	789	kg/m^3
Cp/Hv	0.0044	
Height of liq	45	
Diameter	5	mm
MW	46.068	g/mol
Tank Capacity	100	Liters
ERPG-1	1800	
ERPG-2	3300	
ERPG-3		
Step 1 (Liquid Release Rate L)	0.44450606	
Step 2 (Total Liquid Released. WT)	400.0554538	
Step 3 (Fraction flashed. Fv)	-0.234476	
Step 4 (Pool Size. Wp)	869.0724668	
Pool Area (Ap)	110.1486016	
Step 4 (Airborne Quantity from Flash AQf)	0.44450606	
Step 5 (Airborne Quantity Evap from Pool AQp)	1.041292479	
Step 6 (Total Airborne Quantity AQ)	0.44450606	
Step 6	0.44450606	
CEI	7.603078464	
CEI	7.603078464	
HD-1	102.9461691	
HD-2	76.03078464	
HD-3	N/A	

7.4 Appendix 4: Impurities in zinc acetate dihydrate

The ZnO holds several impurties due to the fact that the source material for zinc is zinc acetate dihydrate, which contains the follwing impurities:

Table 7: Impurities present in zinc acetate dihydrate

Compound	maximum limits (%)
Insoluble matter	0.003
Chloride	0.001
Nitrogen compounds	0.002
Sulphate	0.005
Arsenic	0.00004
Cadmium	0.001
Calcium	0.01
Cupper	0.001
Iron	0.003
Lead	0.001
Manganeese	0.001
Pottasium	0.01
Sodium	0.005

Some of these impurities may be transferred over to the film layer and has a low itensity so the XRD will not catch them but may influence film properties.